PAPER

Hubble distancing: focusing on distance measurements in cosmology

Journal of Cosmology and Astroparticle Physics
An IOP and SISSA journal

Hubble distancing: focusing on distance measurements in cosmology

Kylar L. Greene and Francis-Yan Cyr-Racine

Department of Physics and Astronomy, University of New Mexico,
210 Yale NE, Albuquerque, NM 87131, U.S.A.

E-mail: kygreene@unm.edu, fycr@unm.edu

Received January 10, 2022
Revised April 29, 2022
Accepted April 29, 2022
Published June 7, 2022

Abstract. The Hubble-Lemaître tension is currently one of the most important questions in cosmology. Most of the focus so far has been on reconciling the Hubble constant value inferred from detailed cosmic microwave background measurement with that from the local distance ladder. This emphasis on one number — namely H_0 — misses the fact that the tension fundamentally arises from disagreements of distance measurements. To be successful, a proposed cosmological model must accurately fit these distances rather than simply infer a given value of H_0. Using the newly developed likelihood package '*distanceladder*', which integrates the local distance ladder into `MontePython`, we show that focusing on H_0 at the expense of distances can lead to the spurious detection of new physics in models which change late-time cosmology. As such, we encourage the observational cosmology community to make their actual distance measurements broadly available to model builders instead of simply quoting their derived Hubble constant values.

Keywords: cosmology of theories beyond the SM, dark energy theory, supernova type Ia — standard candles

ArXiv ePrint: 2112.11567

https://doi.org/10.1088/1475-7516/2022/06/002

JCAP06(2022)002

Contents

1 Introduction **1**

2 Distance measurements in cosmology **3**
2.1 The distance ladder 3
2.1.1 Anchor measurements 3
2.1.2 Calibrating standard candles 5
2.1.3 SNe Ia 6
2.2 CMB distance measurements 7
2.3 Strong lensing cosmography 7

3 The *distanceladder* likelihood **8**
3.1 Implementation and usage 9
3.2 Consistency with previous results 10
3.3 A new metric to assess the tension between data sets 11
3.4 Equivalence with Gaussian prior for early-time dynamics 13

4 Models impacting late-time cosmology: issues with Gaussian H_0 prior **14**
4.1 Test case: a sudden dark energy transition at late times 15
4.1.1 Model setup 15
4.1.2 Taking into account the distance measurements: results 16
4.2 Discussion 18

5 Conclusion **19**

A Distanceladder vs. Gaussian prior on $M_{\rm sn}$ **20**

JCAP06(2022)002

1 Introduction

The pioneering work of Slipher, Lemaître, Robertson, Leavitt, and Hubble in the late 1920s established that the Universe is expanding [1–5]. Since then, cosmological distance measurements have been at the forefront of understanding the expansion history of the Universe. Measuring astronomical distances is not a trivial task. Every cosmological distance measurement relies on establishing an absolute *dimensionful* length scale that other distance measurements are then compared to. Fortunately, we live in a Universe where multiple such absolute distances are available: photon-baryon sound horizon [6–10], parallax distances to nearby stars [11–13], distances to eclipsing binaries [14–16], distances to water masers [17–19], and time-delay distances to strong gravitational lenses [20–22].

However, there exists a tension between the various absolute distance scales used to infer the Hubble constant H_0 within the standard Λ cold dark matter (ΛCDM) model [23–28]. Most notably, cosmic microwave background (CMB) measurements [29–31] and the Cepheid-calibrated local distance ladder [32–36] infer Hubble constant values that are discrepant at the critical 5σ level [37]. On the other hand, an alternative calibration of the local distance ladder based on the tip of the giant branch (TRGB) [38–48] leads to a Hubble constant

value that is somewhat intermediate between that inferred from the CMB and the Cepheid-calibrated ladder, while strong-lensing time delays [49–52] generally find H_0 values that are consistent with the Cepheid-calibrated distance ladder, albeit with larger possible systematic errors [53]. A major question in cosmology now is whether this discrepancy is the result of a yet-to-be-discovered systematics or is caused by a breakdown of our current cosmological paradigm [54–56].

Reference [57] summarizes many possible new-physics solutions to alleviate the tension, while ref. [58] ranks the proposed models with respect to a common data set. Generally speaking, new-physics scenarios can be classified into two broad categories, depending on whether they primarily modify the early or late Universe. Early-time solutions aim to decrease the value of the sound horizon r_s [6–10], either by injecting energy into the pre-recombination Universe (see e.g. refs. [59–78]) or by other means [79–82] in such a way that also preserves the CMB measurements. Late-time solutions aim to increase the value of H_0 locally by modifying the expansion history at $z \lesssim 1$ (see e.g. refs. [83–116]). At face value, these late solutions may appear to resolve the tension because a sudden increase in the Hubble expansion rate at very-late times could yield a larger apparent H_0 value while only causing a small fractional change in the overall distance to the CMB last-scattering surface. However, such solutions are misleading in the notion that the local distance ladder *directly* measures the Hubble expansion rate at $z = 0$ [27]. In practice, the local distance ladder infers H_0 from measurements of the peak absolute type Ia supernova (SNe Ia) magnitude $M_{\rm sn}$ and of Hubble flow SNe Ia with redshift $z \gtrsim 0.02$. To be successful, late-time solutions therefore need to accurately fit the measured distances to Hubble-flow supernovae, rather than trying to obtain a given H_0 value derived using ΛCDM assumptions.

Indeed, the singular focus on H_0 rather than on the calibrated distances to Hubble flow objects often obscures what model ingredients are necessary to address the root cause of the discrepancy [25, 117–121]. In cosmological models that are phenomenologically close to ΛCDM at late times (including models that only affect the early Universe), this focus on H_0 is warranted as distances to Hubble-flow objects are inversely proportional to the Hubble constant, and the cosmographic expansion of the luminosity distance is accurate at low redshifts. For these, using a Gaussian prior on H_0 to represent the entire distance ladder is likely sufficient, albeit at the price of discarding information about the actual goodness of fit of model distances to low-redshift objects. On the other hand, for cosmologies that differ significantly from ΛCDM at late times, the relationship between H_0 and distances is more complex as other model parameters could enter the computation of the latter. In this case, simply focusing on H_0 can be extremely misleading as it is not possible to boil down the entirety of the distance ladder to a single number without important loss of information. Instead, the distances to Hubble-flow objects must be directly accounted for in assessing the success of such cosmological scenarios.

In this paper, we show that the Hubble-Lemaître tension is not simply about a single number — namely H_0 — but rather about a large array of distance measurements at low redshifts. In this language, "solving" this discrepancy is really about finding a self-consistent expansion history of the Universe that can describe all cosmological data, including the CMB, large-scale structure, Big-Bang Nucleosynthesis abundance yields, baryon acoustic oscillation, and the distances to nearby Hubble-flow objects such as SNe Ia and strong lenses. Using the newly developed likelihood package *distanceladder*,[1] which provides a fast yet accurate fit to

[1]The package is publicly available at distanceladder.

JCAP06(2022)002

the entirety of the local distance ladder, we show that apparently promising late-time solutions that have been presented in the literature, in fact, provide poor fits to the actual measured distances to low-redshift objects. Even more concerning, we show that some evidence for new physics that has been reported in the literature using a Gaussian H_0 prior appears to be spurious once the actual distance measurements are properly taken into account. Our work strongly indicates that cosmological analyses should focus on fitting cosmological distances rather than argue about the "correct" value of the current expansion rate.

This paper is structured as follows. Section 2 discusses the various methods in which distances are measured locally and the absolute dimensionful scale they establish. It also reviews how the local distance ladder is built. Section 3 presents the details of the *distance-ladder* package we have developed to correctly analyze changes to late-time cosmology and also present the various consistency checks that we have performed. In section 4, we use this likelihood package to demonstrate that a simple Gaussian H_0 prior cannot capture the complexity of the entire local distance ladder and can even lead to spurious detection of new physics. We finally conclude in section 5.

2 Distance measurements in cosmology

In cosmology, any distance measurement depends on first establishing an absolute dimensionful anchor that defines the problem's overall scale. Such anchors do not necessarily need to be absolute distance scales, but can also be a time interval, the linear size of an object, an acceleration, or a temperature, among others. What they all have in common is that they establish a dimensionful scale from which a distance can eventually be measured. In the following, we briefly review different distance measurement techniques in cosmology, highlighting the absolute *dimensionful scale* anchoring each approach, and describe the logical flow from that anchor to the inferred cosmological distances. Our goal here is to provide a concise end-to-end description of the distance measurements that are instrumental to the existence of the Hubble-Lemaître Tension. As such, we focus below on the local distance ladder, the cosmic microwave background, and strong gravitational lensing cosmography. Other important techniques include cosmic chronometers [122–128], gravitational wave standard sirens [129–133], surface brightness fluctuations [134–139], Tully-Fisher relation [140–146], Type II supernovae [147–152], and HII galaxies [153–156].

2.1 The distance ladder

2.1.1 Anchor measurements

In cosmology, distance ladders are built by establishing the absolute distance to nearby stars or galaxies. Such distances usually referred to as anchors, are derived from measurements of other absolute dimensionful scales. Common methods of measuring the distance to these anchors include stellar parallax [157–163], detached eclipsing binary stars [14, 164–167], and MASER emission from the accretion disk of super-massive black holes [17, 18, 168–172]. We briefly describe these below, noting the key dimensionful scales entering the problem in each case.

Parallax. The modern parallax method measures the apparent movement of a stellar object with respect to the background stars on the sky as the Earth revolves around the sun. Because the star is very far away compared to the perceived motion of the star on the night sky, the

JCAP06(2022)002

parallax equation is simply

$$d = \frac{1}{p}, \tag{2.1}$$

where d is the distance in parsecs, and p is the parallax angle measured in arcseconds. The absolute *dimensionful scale* for the modern parallax method is the baseline distance established between two observations, typically the diameter of Earth's orbit. This is a precisely measured value known as an astronomical unit (AU) equivalent to $149,597,870,700 \pm 3$ meters [173, 174]. While parallax measurements are highly precise, they are severely limited in the measurable distance, with the furthest measurements reaching the Milky Way's galactic centre using the Gaia space telescope [12, 175–177].

Detached eclipsing binaries. The Detached Eclipsing Binary (DEB) method utilizes binary stars whose orbit takes the pair within the observer's line of sight, resulting in primary and secondary eclipses [14, 15, 166, 178–180]. Here, the pair's "detached" nature means that the binary stars' separation is much larger than their individual radii, which avoids complications related to mass transfer and accretion disks. The absolute *dimensionful scale* entering the problem is the orbital period of the binary pair, which can be measured both from the light curve and from radial velocity spectroscopic data. These observations can also be used to measure the inclination and eccentricity of the DEB system's orbit, which, when combined with the orbital period measurement, allows one to determine the orbital radius from Kepler's laws. Then, the shape of the primary and secondary eclipses can be used to calculate the radius of each star. Finally, spectroscopic and color information is used to estimate the surface brightness of each star, which can be used to compute the distance to the pair

$$d = \left(\frac{F_1}{F_{1,\mathrm{tel}}}\right)^{1/2} R_1 = \left(\frac{F_2}{F_{2,\mathrm{tel}}}\right)^{1/2} R_2 \tag{2.2}$$

where F_i is the flux from each star, $F_{i,\mathrm{tel}}$ is the flux received at the telescope, and R_i is the radius of that star determined using the method outlined above. The two estimates for d in eq. (2.2) provide a vital consistency check for the distance measurement. This procedure can also be carried in multiple photometric bands, providing further cross-checks of the distance estimate. The assumptions surrounding the surface brightness estimate of each star represent the most significant potential systematics of the DEB technique. However, previous work has demonstrated consistent models for surface brightness with negligible dependence on metallicity effects [181, 182]. Additionally, the systems are difficult to detect due to their detached nature, causing transits to be very short, which limits the number of available distance measurements [14].

MASERS. Super-massive black holes (SMBH) heat the surrounding gas in their accretion disk to very high temperatures, producing x-ray emission. This strong radiation field can stimulate various molecules present within the disk, particularly that of water, resulting in localized MASER emission [183–187]. Such MASERs are high intensity and point-like, allowing for line-of-sight (LOS) velocities to be measured in the accretion disk within thousands of Schwarzchild radii of the SMBH. Furthermore, the orbital speed of the MASERs around the central engine is large enough that their LOS acceleration can also be measured over a few years. Once the LOS acceleration, LOS velocity, and velocity gradient are measured, a

JCAP06(2022)002

distance can be determined according to

$$d = \frac{\partial_\theta v_{\rm LOS}}{a_{\rm LOS}} v_{\rm LOS} \tag{2.3}$$

where $v_{\rm LOS}$ is the LOS velocity, θ is the angle on the sky according to the observer, $\partial_\theta v_{\rm LOS}$ is the LOS velocity gradient on the sky, and $a_{\rm LOS}$ is the LOS acceleration [188]. In this case, the absolute *dimensionful scale* established by the MASER method is the LOS acceleration. The MASER method additionally can directly measure distances into the Hubble flow, notably by the Megamaser Cosmology Project who directly measure from distances to be $H_0 = 73.9 \pm 3.0$ km/s/Mpc [18]. However, current systematic errors associated with radio phase calibration make the MASER method challenging to perform [189]. Additionally, the small number of known MASERS with nearby phase calibrators limits the method's applicability.

2.1.2 Calibrating standard candles

The second step of the distance ladder depends on calibrating standard candles. These calibrators must satisfy the following criteria; (i) have anchor measurements of their distance from us using one of the techniques outlined in section 2.1.1, and (ii) exist in a host galaxy with other, brighter standard candles (such as SNe Ia) that are observable in the Hubble flow. While we focus below on cepheids and the tip of the red giant branch, we note that mira variable and RR Lyrae stars have also been used as calibrating standard candles [190–194].

Cepheid variable stars. Leavitt's law gives a relationship between the period and apparent magnitude of a Cepheid variable star [1]. Once anchor measurements determine the distance to a subsample of Cepheids, Leavitt's Law can be calibrated. Then, the apparent magnitude of a hypothetical Cepheid star with a one day-long period is calculated using linear regression. The absolute magnitude of Cepheids, $M_{\rm ceph}$, is determined by the distance modulus equation using the anchor distance measurement of a Cepheid and the apparent magnitude of the hypothetical one day period Cepheid. In terms of magnitude, the distance modulus μ is given by

$$\mu = m - M \tag{2.4}$$

where m is the apparent magnitude and M is the absolute magnitude. Then, the apparent magnitude of a hypothetical one day period Cepheid in a nearby host galaxy is calculated using observations of Cepheid populations. Finally, the distance to the host galaxy is calculated from equation (2.4) using $M_{\rm ceph}$ and the calculated apparent magnitude of a one day period Cepheid in the same host galaxy. Recently, the nature of Leavitt's Law has come under question as the relationship between period and magnitude for Cepheids may not be wholly linear but have a 'break' where the slope changes value [195–197]. Additionally, metallicity effects on the star may change the period to luminosity relationship, although previous studies have found the overall effect from metalicity to be small [198, 199].

Tip of the red giant branch. Red giant branch stars are old, evolved stars with an inert helium core. Once the inert helium core reaches conditions to allow for fusion, it ignites in a highly energetic event and expels a large amount of matter from the star's atmosphere, leading to an immediate decrease in luminosity. This behaviour leads to the 'tip of the red giant branch' (TRGB) as a standard candle, as the helium flash will occur at similar mass conditions for all red giant branch stars [200]. The peak absolute magnitude of the tip, $M_{\rm TRGB}$, is calculated by the CCHP (Carnegie-Chicago Hubble Program) and Freedman (2021)

JCAP06(2022)002

(hereafter referred to as F21) in a three-step process [38–44, 46, 48]. First, a large sample of potential red giant branch stars from the same galaxy undergoes a selection cut based on colour to remove other evolved stars. Second, the luminosity function is determined from the cut sample. Third, a Sobel edge detection filter is used to determine the edge of the luminosity function, which corresponds to the TRGB. Once $M_{\rm TRGB}$ is calculated and calibrated with an anchor measurement (using one of the techniques described in section 2.1.1), the TRGB can be used to determine the distance to SNe Ia host galaxies much in the same way that other calibrating standard candles do. However, only observations of the halo's of galaxies should be used to calculate $M_{\rm TRGB}$ as the inner regions of galaxies will have asymptotic giant branch stars which contaminate the sample [46].

2.1.3 SNe Ia

The final rung of the distance ladder's involves SNe Ia. SNe Ia occurs in binary systems in which a white dwarf is actively accreting material from its binary companion. Eventually, the electron degeneracy pressure can no longer support the mass of the white dwarf, and the Chandrasekhar mass limit [201] is reached (approximately equal to 1.44 $M_\odot$), at which point the white dwarf collapses, and a supernova occurs. These are excellent standard candles for measuring distances well into the Hubble flow because the mass at which these supernovae occur is consistent and the event's magnitude bright.

Local SNe Ia. Measuring the absolute magnitude of SNe Ia, $M_{\rm sn}$, requires measurements of SNe Ia in the same host galaxy as calibrating standard candles [202, 203], such as cepheids or TRGB stars. Because the distance to the host galaxy is much greater than the host galaxy's size, it is assumed that the calculated distance modulus of the calibrating standard candle is the same as the SNe Ia. Ref. [46] describes 18 recorded SNe Ia occurring in galaxies in which TRGB measurements are available, while ref. [37] describes 42 recorded SNe Ia occurring in galaxies in which Cepheid data are available.

Hubble flow SNe Ia. The distance modulus to distant SNe Ia well into the Hubble flow is then measured using $M_{\rm sn}$ and apparent magnitude measurements. These distant SNe Ia also have redshift measurements, enabling a distance modulus-redshift relationship to be defined, which in terms of luminosity distance is given by

$$\mu = 5\log(d_{\rm L}) + 25, \tag{2.5}$$

where d_L is the luminosity distance in Mpc which is given by

$$d_{\rm L} = (1+z)\frac{c}{H_0}\int_0^z \frac{dz'}{E(z')}, \tag{2.6}$$

and $E(z) = H(z)/H_0$ is the dimensionless Hubble rate. Therefore, we can solve eq. (2.4) for H_0 in terms of only observable quantities to find

$$\mu \propto \log_{10}\left(\frac{c}{H_0}\int_0^z \frac{dz'}{E(z')}\right). \tag{2.7}$$

Equation (2.7) explicitly shows that distance measurements determine the value of H_0. Indeed, calculating H_0 at $z = 0$ from the local distance ladder relies on distance measurements of SNe Ia in the redshift range $z \gtrsim 0.02$, with the lower bound set to avoid the coherent flow of local SNe Ia [34]. Additionally, the overall shape of the redshift-luminosity relationship is relevant due to the redshift integral in eq. (2.6) [26].

JCAP06(2022)002

2.2 CMB distance measurements

The most precise measurements of the Hubble constant have so far been obtained from detailed observations of the CMB [29]. Light from the CMB last-scattering surface forms a two-dimensional projected map on the sky whose primary observables are temperature and polarization fluctuations on different angular scales. These perturbations tell us about critical physical processes in the pre-recombination era. By themselves, fractional temperature and polarization fluctuations seen projected on the sky do not set an absolute distance scale from which the Hubble constant can be inferred [65]. What fundamentally allows us to determine H_0 from CMB observations in the ΛCDM model is the knowledge of the CMB temperature today T_0, which provides an *absolute scale* on which cosmological distances important to the CMB can be calibrated [204].

The most prominent CMB angle on the sky is the angular size of the sound horizon at last scattering ($z_\star$), which is given by

$$\theta_\star = \frac{r_\mathrm{s}}{D_\mathrm{A}(z_\star)}, \tag{2.8}$$

where r_s is the comoving baryon-photon sound horizon, and $D_\mathrm{A}(z_\star)$ is the comoving angular diameter distance to the CMB. Mathematically, r_s and $D_\mathrm{A}(z_\star)$ are given by

$$r_\mathrm{s} = \int_{z_\star}^{\infty} \frac{c_\mathrm{s} dz}{H(z)} \quad \text{and} \quad D_\mathrm{A}(z_\star) = \int_0^{z_\star} \frac{dz}{H(z)}, \tag{2.9}$$

where c_s is the sound speed of the primeval plasma, and $H(z)$ is the Hubble expansion rate. On dimensional ground, the comoving sound horizon is approximately given in ΛCDM by $r_\mathrm{s} \simeq 10^{-4} M_\mathrm{pl}/T_0^2$, where M_pl is the Planck mass and the prefactor has mild dependence on the redshift of matter-radiation equality, the photon-to-baryon ratio, and $z_\star$. On the other hand, the comoving angular diameter distance scales as $D_\mathrm{A}(z_\star) \simeq (3.1 H_0)^{-1}$, which implies that the Hubble constant inferred in ΛCDM by the CMB is approximately

$$H_0 \sim 3.1 \times 10^4 \theta_\star \frac{T_0^2}{M_\mathrm{pl}}. \tag{2.10}$$

While precise measurements of the anisotropies on the CMB give a measurement of $\theta_\star$ to an accuracy of 0.03% [29], uncertainties in other (dimensionless) cosmological parameters entering the prefactor in eq. (2.10) result in the CMB measuring H_0 to a 0.8% precision within ΛCDM.

2.3 Strong lensing cosmography

Gravitational lensing cosmography offers a critical check of distance measurements, as lensing distances can directly probe distances well into the Hubble flow and are independent of the local distance ladder and the CMB [49–53]. Strong gravitational lensing occurs when a significant mass distribution is in the line of sight between the observer and the source, which results in the appearance of multiple images of the background source [205]. If the source is variable such as a quasar, we can measure the time delay difference, Δt_AB, between the light curves of the different images as the light takes different paths to the observer. This time interval forms the *absolute scale* in the problem and is given by

$$\Delta t_\mathrm{AB} = \frac{D_{\Delta \mathrm{t}}}{c} \left(\phi(\theta_\mathrm{A}, \beta) - \phi(\theta_\mathrm{B}, \beta) \right), \tag{2.11}$$

JCAP06(2022)002

where $D_{\Delta t}$ is the time delay distance, ϕ are Fermat potentials, θ is the image location, and β is the corresponding source position relative to an unperturbed path. The time delay distance then is defined by

$$D_{\Delta t} = (1 + z_d)\frac{D_d D_s}{D_{sd}}, \tag{2.12}$$

where z_d is the redshift of the gravitational lens, D_d is the angular diameter distance to the lens, D_s is the angular diameter distance to the source, and D_{sd} is the angular diameter distance from the lens to the source [206]. From this, we see that

$$D_{\Delta t} \propto \frac{c}{H_0}. \tag{2.13}$$

So far, a sample of 8 quasar lenses has been used to infer the Hubble constant using this technique. This sample is expected to grow significantly in the near future with the advent of wide surveys enabled by the Vera Rubin Observatory, and the Euclid satellite [207–209]. A major challenge for the method remains the accurate determination of the lensing mass models for each target and the proper modelling of line-of-sight effects [210]. Additionally, strong lensing cosmography requires a significant amount of observation time to determine the time delay accurately [211]. In the past, several years of data were required to overcome microlensing variability and obtain reliable time delays, but recent studies have shown that a year of daily observations could be sufficient [212, 213]. In any case, the cadence of the Legacy Survey of Space and Time at the Rubin Observatory [214–216] is expected to yield a sizable sample of lensing times delays that will be used for cosmography, bringing this technique well into the systematics-dominated regime.

3 The *distanceladder* likelihood

In a significant number of cosmological analyses to date for late-time changes to cosmology (see e.g. refs. [87, 101, 103, 106, 107, 114, 217–220]), all of the richness and complexity of the distance ladder measurements described in the previous section are reduced to a simple Gaussian constraint on H_0 (see refs. [89, 121] for exceptions to this). However, such Gaussian prior on the $z = 0$ Hubble rate is an obvious over-simplification since it neglects that all of the information on the expansion rate gathered from the distance ladder comes from redshifts higher than zero. In particular, all information on the shape of the SNe Ia magnitude-redshift relation is lost when boiling down the whole distance ladder to a simple Gaussian prior on H_0 [27, 221]. It is thus worth emphasizing that to resolve the Hubble-Lemaître Tension; it is in general *not* sufficient for a cosmological model to have a $z = 0$ Hubble rate compatible with the value reported by the distance ladder measurements. Instead, the model must be able to successfully fit the *calibrated distances* to SNe Ia in the Hubble flow. Indeed, while there is a one-to-one relation between distances and the Hubble constant for ΛCDM models with fixed acceleration and jerk parameters q_0 and j_0 [84], this is in general not the case for models with a sudden late-time transition for which the cosmographic expansion of the luminosity distance breaks down. Such theories can appear to resolve the tension by having a Hubble constant compatible with that inferred from the distance ladder but do not necessarily provide a good fit to the actual supernova distances.

To remedy this, we introduce here the *distanceladder* numerical likelihood package, which replaces the standard Gaussian prior on H_0 (or M_{sn}) used in many analyses with a direct fit to the calibrated distances of the SNe Ia in the Hubble flow. Our goal here is not to

JCAP06(2022)002

replace the detailed analyses performed in, e.g., refs. [32, 34, 37, 46], but instead provide the user with an end-to-end distance-ladder package such that the impact of different analysis assumptions and choices on cosmological constraints can be fully understood. We briefly describe below the content of the numerical package and its usage and then illustrate in section 4 how a model that appears to resolve the Hubble-Lemaître Tension can be strongly disfavored once the actual distances are taken into account, using a dynamic late-time dark energy (LDE) model as a case example. For the remainder of this discussion, when a Gaussian prior is used, it utilizes the results of R21 with $H_0 = 73.2 \pm 1.3$ km/s/Mpc.

3.1 Implementation and usage

As its core, the '*distanceladder*' likelihood package incorporates the local distance ladder as described by section 2.1 into the Monte-Carlo-Markov-Chain tool `MontePython` [222] by directly comparing the measured luminosity distances of Hubble flow SNe Ia to the distances predicted by a cosmological model. The *distanceladder* nullifies the need for a Gaussian prior on H_0 and allows all cosmological models, even those with baroque late-time dynamics, to properly account for the distances measured by the local distance ladder.

User inputs. *distanceladder* requires two inputs from the user; a choice of calibrating standard candles and a choice of anchor measurements. The available options of calibrating standard candles are Cepheids, the TRGB, or a subsample in which the distances to anchor SNe Ia calculated by both methods agree to 1σ referred to as the 'concordant' sample. The concordant option allows the user to select the SNe Ia anchors which agree on distance measurements between the TRGB and the Cepheid calibration providing a unique tool to analyze the tension seen between the two methodologies. The choice of anchors is only available for the Cepheid calibration presently. A future update will include the 42 Cepheid calibrators [37] as well as the Pantheon+ sample for Hubble flow SNe Ia [223, 224]. Additionally, future iterations may include an option to use the Carnegie Supernova Project (CSP) Hubble flow SNe Ia data [225] as the Hubble flow supernova data, if there is interest from the community.

Calibrating standard candles. If Cepheids are chosen as the calibrating standard candle of choice, $M_{\rm ceph}$ is first calculated based on the choice of anchors. Currently, the LMC and NGC4258 are supported as anchor choices. The distance to the anchors are provided directly and are not recalculated, using the results of ref. [178] for the LMC and ref. [17] for NGC4258. If both anchors are chosen, $M_{\rm ceph}$ is calculated independently for both anchors then combined using a weighted average using data from refs. [226, 227]. Once $M_{\rm ceph}$ is calculated, the weighted average slope of Leavitt's Law is determined using the Cepheid data directly from the 19 host galaxies presented by ref. [34] in the Wesenheit near-infrared magnitude band [228]. The correlation value R between Cepheid intrinsic colour and luminosity is assumed to be $R = 0.386$ as done by SH_0ES. Using the Copernican principle, the *distanceladder* assumes that all Cepheids in the data sample provided will have identical slopes. The global slope of Leavitt's Law is then applied to the Cepheid samples of the 19 SNe Ia host galaxies to determine the intercept of the relation. As discussed previously, there may exist a break in Leavitt's law in which case this method can be generalized to include a broken power-law feature in the future. The distance modulus given by eq. (2.4) determines the distance to the host galaxies by using $M_{\rm ceph}$ and the intercept of Leavitt's Law for each host galaxy. Finally, a linear regression calculates the intercept of the relation between the distance to the

JCAP06(2022)002

host galaxies and SNe Ia's apparent magnitude. The intercept corresponds to the absolute magnitude of SNe Ia, $M_{\rm sn}$.

If the TRGB is chosen as the calibrating standard candle of choice, the distance modulus to the host galaxies is not calculated by the likelihood package but instead taken from table 3 from ref. [46]. The TRGB method of calculating distances is more involved than the Cepheid method, so it is not explicitly included in this release but may be included in future releases if there is interest. A linear regression using the distance modulus from table 3 of ref. [46], and the apparent magnitude of the local SNe Ia calculates $M_{\rm sn}$ in the same manner as in the Cepheid method. In all calculations, the Hubble photometry B magnitudes are used as the standard filter of choice.

If the concordant sample is chosen as the calibrating standard candle, the distance modulus again is not calculated but instead taken from table 3 of ref. [46]. Only distance measurements in which the TRGB and Cepheid calibration agree to less than 1σ are considered. This cut results in a smaller sample size of 6 local SNe Ia than the 19 local SNe Ia calibrated by Cepheids or the 18 local SNe calibrated by the TRGB. $M_{\rm sn}$ is then calculated in the same manner as in the prior two methods.

SNe Ia and tension calculation. Regardless of calibration method, eq. (2.4) calculates the distance to Hubble flow SNe Ia using $M_{\rm sn}$ and apparent magnitude measurements from the Pantheon data set [229]. Since our analysis does not rely on the cosmographic expansion of the luminosity distance, the *distanceladder* uses the *entire* Pantheon dataset with no upper bound on redshift to ensure the shape of the redshift-luminosity relationship is fully accounted for. Separately from the *distanceladder* likelihood, the Boltzmann code CLASS [230] then calculates the luminosity distances to these Hubble flow SNe Ia for the cosmological model under consideration. The Hubble-Lemaître Tension (if present in the model) is then quantified as a disagreement of distances, not of H_0 values, by comparing the distance moduli of the Hubble flow SNe Ia calculated from $M_{\rm sn}$ to those inferred from the cosmological model.

Redshift errors. Redshift errors are included whenever possible for the Hubble flow supernovae from ref. [231]. Not all supernovae in Pantheon have errors that are available presently (this has been changed in the recent Pantheon+ release [223]). The average fractional error of the 831 supernovae with errors available in the overall Pantheon data set is 0.83%. The average fractional error of the 184 supernovae with errors available with $z < 0.15$ (corresponding to the upper redshift cut of R21 and similar studies) in the Pantheon data set is 1.0%. While the fractional error is small, the redshift error does need to be incorporated in future studies. The covariant matrix used by *distanceladder* in minimizing the distance disagreement is generated by adding the observational errors associated with apparent magnitude and redshift as a diagonal matrix to a dense matrix where each element is the error associated with $M_{\rm sn}$, representing the systematic error.

3.2 Consistency with previous results

As a consistency check, figure 1 demonstrates the ability of the *distanceladder* likelihood to recover the results of both the F21 and R21 for a ΛCDM model using the Monte-Carlo Markov Chain tool `MontePython`. The ΛCDM model utilizes Planck high-ℓ TTTEE, low-ℓ EE, and low-ℓ TT data to represent the cosmological measurement of H_0. The local measurements utilize the *distanceladeer* likelihood with the respective calibration choice and a prior on the baryon density to represent the local measurement of H_0. The TRGB calibration accurately recovers the F21 mean value result but underestimates the error slightly as the larger Pantheon

JCAP06(2022)002

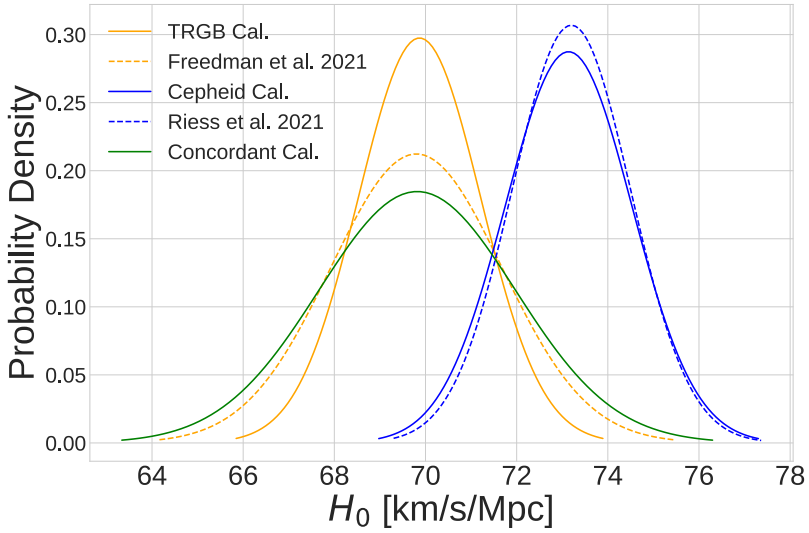

Figure 1. 1D posterior distributions of H_0 using only the *distanceladder* likelihood, comparing the user input choices of using the TRGB, Cepheid, or concordant calibration. The solid lines correspond to *distanceladder* results using the tip of the red giant branch calibration (yellow), Cepheid calibration (blue), or a combination of the results in which both calibration schemes agree on the host galaxy distances (green). The dashed lines correspond to the previous results obtained by ref. [46] (yellow) and ref. [36] (blue).

supernova data set in B magnitude is used, rather than the smaller CSP data set in the B′ magnitude, which uses a different photometric calibration scheme and different assumptions of blackbody physics. However, because we can reproduce the mean results of the F21 study nearly precisely using the Pantheon Hubble flow supernovae with B magnitude photometry and the photometric results of ref. [34] for the anchor supernova, the results support that the CSP and Pantheon supernovae data sets are mostly consistent and do not contribute to the tension nor does the photometry of ref. [34]. The Cepheid calibration recovers an accurate mean value of H_0 compared to the R21 value, with the slight difference stemming from the *distanceladder* likelihood only having access to the LMC and NGC4258 as anchors while the R21 value uses the LMC, NGC4258, and Milky Way Cepheids as anchors. Interestingly, the concordant sample finds a value of H_0 similar to the F21 result with larger error bars due to less anchor SNe Ia available, which should be investigated in future studies.

Table 1 summarizes the values of $M_{\rm sn}$ and H_0 for our different calibration choices in a ΛCDM model. An unexpected behaviour of the results is that when increasing the error in $M_{\rm sn}$ as seen in the Concordant sample case, a smaller value of H_0 is preferred from the MCMC breaking the typical relationship between H_0 and $M_{\rm sn}$. As a check to determine if it was indeed the error in $M_{\rm sn}$ driving this difference, we reran the concordant calibration scheme artificially lowering the error in $M_{\rm sn}$ by a factor of 2. By forcing the error in $M_{\rm sn}$ to be similar to that seen in the Cepheid and TRGB calibration schemes, we find that the typical relationship between $M_{\rm sn}$ and H_0 is recovered.

3.3 A new metric to assess the tension between data sets

Now that we a have likelihood focusing on cosmological distances rather than H_0 itself, the next question is which metric should be used to compare local distance measurements with predictions from high-redshift observations such as the CMB? The intercept β presented in

JCAP06(2022)002

	Cepheid Cal.	TRGB Cal.	Concordant Cal.
$M_{\rm sn}$	-19.226 ± 0.039	-19.325 ± 0.039	-19.267 ± 0.064
H_0	73.14 ± 1.39	69.87 ± 1.34	69.82 ± 2.16

Table 1. The distance ladder parameters derived from *distanceladder* for the three calibration options available. $M_{\rm sn}$ is given in the B apparent, K corrected peak magnitude. H_0 is given in units of km/s/Mpc. The concordant sample finds a value of H_0 similar to the TRGB calibration at the cost of increasing the error nearly two-fold.

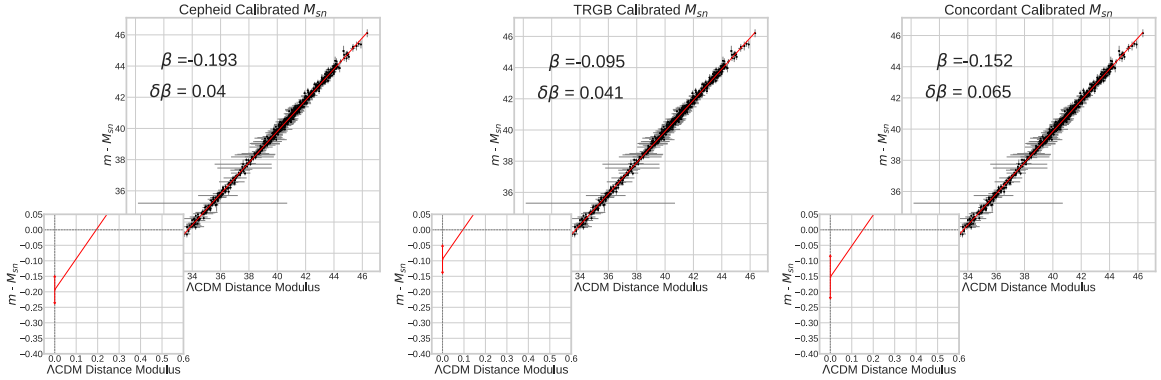

Figure 2. (left) Graph comparing the calculated distance moduli for Hubble flow supernova. The y-axis describes the distance modulus as calculated by the local distance ladder using the $M_{\rm sn}$ absolute distance scale, calibrated by Cepheid variable stars. The x-axis describes the distance modulus as calculated from Planck CMB measurements assuming a ΛCDM model. (middle) Graph describing an identical situation as in the previous panel but using the TRGB method to calibrate $M_{\rm sn}$. (right) Graph describing an identical situation as in the previous two panels, but using the concordant calibration for $M_{\rm sn}$.

figure 2 may be what future studies should focus on to resolve the Hubble-Lemaître Tension, rather than H_0 itself. In this figure, the y-axis represents the distance moduli to Hubble flow SNe Ia as inferred by the local distance ladder. The x-axis represents the distance moduli to the Hubble flow SNe Ia as inferred in a ΛCDM cosmological model fitted to Planck data, including errors associated with redshift expansion rate [29]. The intercept β is calculated for the three calibration schemes and ΛCDM using a simple linear regression with a fixed slope of unity. Allowing the slope to vary is possible and will be sensitive to changes in late-time cosmology, as it will modify the shape of the SN-magnitude redshift relationship, potentially detecting geometric inconsistencies.

If no Hubble-Lemaître Tension existed, the distance moduli established by $M_{\rm sn}$ and those inferred from a cosmological fit to the CMB would agree, and the intercept would be statistically consistent with zero. As we can see from figure 3 however, the β values for our three calibration schemes differ from zero at more than 3σ in a ΛCDM model calibrated to Planck CMB measurements, indicating the presence of the well-known Hubble-Lemaître Tension. Additionally, all cases find a slope statistically identical to unity when allowing the slope to vary, indicating no geometric issues. The width of the β posteriors is similar as all three case examples utilize the same Pantheon data set. Beyond just being a parameter in linear regression, the intercept β also has a clear physical meaning: $-\beta$ represents the change to the absolute SNe Ia magnitude necessary to bring the low-redshift distances to supernovae in agreement with those inferred from the CMB.

JCAP06(2022)002

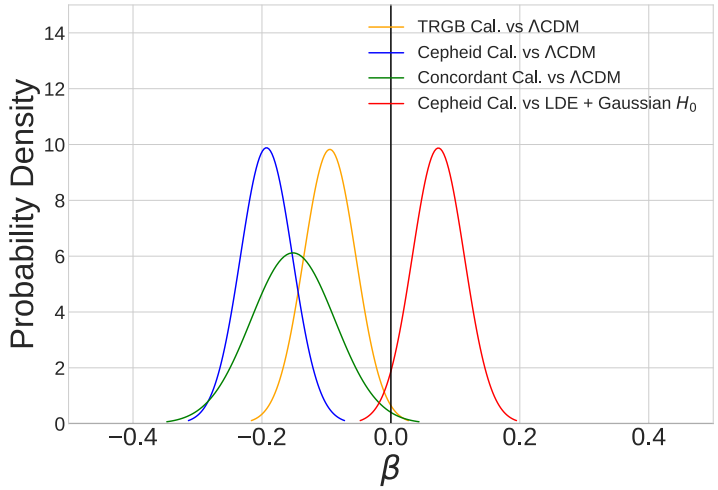

Figure 3. The probability densities of β. The solid black vertical line indicates an agreement between the distance ladder and Planck CMB measurements. The blue, green, and orange lines on the left represent the tension between the chosen calibration scheme and a ΛCDM calibrated to Planck CMB data. The red line on the left represents the tension between a Cepheid calibration scheme and a late-time dark energy model using a Gaussian H_0 to represent the local measurements of the distance ladder. The Gaussian's are shown out to the 3σ level.

3.4 Equivalence with Gaussian prior for early-time dynamics

As an additional consistency check, we consider a simple extension of ΛCDM in which the parameter $N_{\rm eff}$ is allowed to freely vary. Since $N_{\rm eff}$ is a proxy for the abundance of free-streaming radiation (including neutrinos) at early times [232, 233], it has only indirect impacts (i.e. through parameter degeneracies) on the late Universe. As the late-time cosmology in such an extension is phenomenologically similar to ΛCDM for which the standard cosmographic expansion in terms of q_0 and j_0 is valid, we expect that the standard Gaussian H_0 prior and the *distanceladder* likelihood should find nearly equivalent posterior distribution for the Hubble constant when fitted in combination with CMB data. As such, this model constitutes a simple test case to assess the equivalency of our *distanceladder* likelihood with the standard Gaussian prior on H_0 for cosmological models differing from ΛCDM only through their early-Universe evolution (e.g. ref. [60]).

To perform this test, we run MCMC anlyses with the code `MontePython` [222], letting the 6 standard ΛCDM parameters and $N_{\rm eff}$ vary (as well as necessary nuisance parameters) in the fit. As shown in figure 4, we find that our *distanceladder* likelihood reproduces the results obtained from a Gaussian prior on H_0 when performing a joint analysis with CMB data for this one-parameter extension of ΛCDM. In detail, when combined with Planck high-ℓ TTTEE, low-ℓ EE, and low-ℓ TT data [29], our *distanceladder* likelihood finds $N_{\rm eff} = 3.340 \pm 0.148$ ($H_0 = 69.96 \pm 1.01$ km/s/Mpc), which is to be compared with $N_{\rm eff} = 3.344 \pm 0.149$ ($H_0 = 69.95 \pm 1.02$ km/s/Mpc) when using the Gaussian prior on the Hubble constant. The agreement between the *distanceladder* and the Gaussian H_0 prior, in this case, demonstrates that the latter is sufficient when analyzing models modifying the cosmological expansion history at early times. However, as we will see in the next section, this is generally not the case for models changing the Hubble expansion history at late times.

JCAP06(2022)002

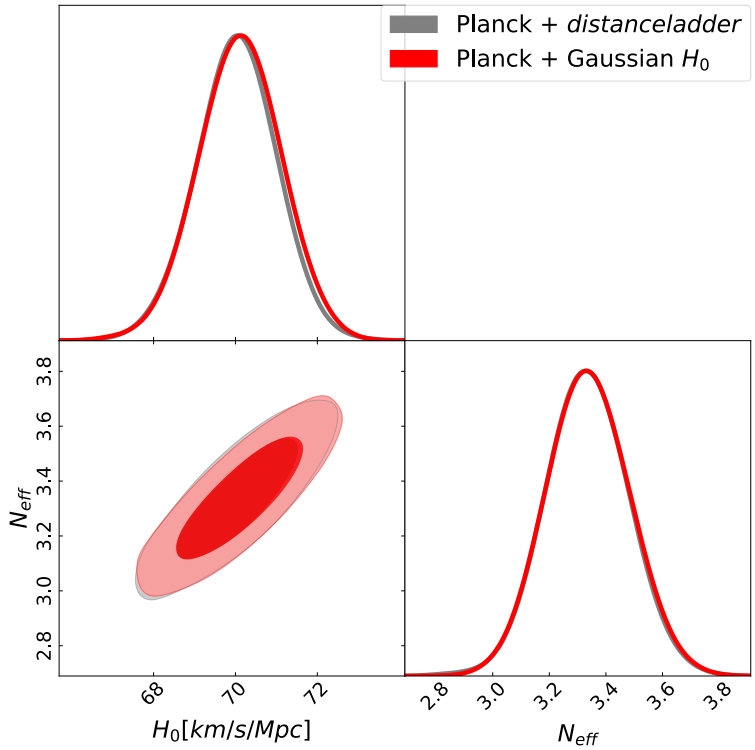

Figure 4. Marginalized posterior distributions for H_0 and $N_{\rm eff}$ using either our *distanceladder* likelihood (DL) or a Gaussian H_0 prior, in combination with Planck temperature and polarization data for both cases [29]. The strong agreement between the *distanceladder* and the Gaussian prior results supports that early-time changes to cosmology only affect distance ladder measurements through H_0.

4 Models impacting late-time cosmology: issues with Gaussian H_0 prior

Our *distanceladder* likelihood package allows one to concentrate on the key issue behind the Hubble-Lemaître Tension: the distances to SNe Ia in the Hubble flow. Refocusing the discussion onto distance disagreements immediately begins to narrow the field of possible solutions to the Hubble-Lemaître tension, specifically those which propose changes to late-time cosmology. Such models may seem at the surface to resolve the tension through their accommodation of larger H_0 values compared to ΛCDM. However, they generally do so at the cost of worsening the tension with the actual distance measurements, indicating that such models do not fundamentally address the root cause of the discrepancy and are therefore only of modest interest.

As an example of how a Gaussian prior on H_0 standing in for the entirety of the local distance ladder can be misleading, we consider below a late-time dark energy (LDE) model in which a sudden transition in the abundance of dark energy increases the value of the Hubble rate close to $z = 0$ [88]. Using our *distanceladder* likelihood package, we show below that such LDE models with a high H_0 value poorly fits the measured SNe Ia distances. While we focus here on this simple phenomenological LDE model, we note that other proposed models such as chameleon dark energy [96, 234] and phenomenological emergent dark energy (see e.g. refs. [235, 236]) will also suffer from this problem.

JCAP06(2022)002

4.1 Test case: a sudden dark energy transition at late times

Prior work has demonstrated that introducing a dynamic component of dark energy, particularly at redshifts $z \lesssim 0.02$, successfully increases the value of H_0 locally while also preserving the CMB temperature and polarization spectra [83, 217]. These solutions generally modify the Friedmann equation to allow for a redshift dependent dark energy density component to be included, such as

$$H^2(z) = H_0^2 \left[\Omega_{\rm r}(1+z)^4 + \Omega_{\rm m}(1+z)^3 + \Omega_{\rm DE} h(z) + \Omega_k (1+z)^2\right], \tag{4.1}$$

$$h(z) = \exp\left[3\int_0^{\ln(1+z)} {\rm dln}(1+z')(1+w_{\rm DE}(z'))\right], \tag{4.2}$$

$$w_{\rm DE} \equiv \frac{p_{\rm DE}}{\rho_{\rm DE}}, \tag{4.3}$$

where $\Omega_{\rm r}$, $\Omega_{\rm m}$, and $\Omega_{\rm DE}$ are the ratio of the current energy density in radiation, matter, and dark energy to the critical density of the Universe. $\Omega_{\rm k}$ is the underlying curvature density parameter, which we set to 0 here to enforce flatness, $p_{\rm DE}$ is the dark energy pressure, and $\rho_{\rm DE}$ is the dark energy density. A subclass of late-time dark energy models which use the above set of equations also allow the phantom regime $w_{\rm DE} < -1$. We remind the reader that the limit of $w_{\rm DE} = -1$ represents the standard cosmological constant.

4.1.1 Model setup

To illustrate how changes to late-time cosmology in the presence of a Gaussian H_0 prior can lead to misleading results, we focus here on the simple phenomenological model presented in ref. [88] in which the dark energy density acquires a time dependence according to

$$\rho_{\rm DE}(z) = [1 + f(z)]\tilde{\rho}_{\rm DE}, \tag{4.4}$$

where

$$f(z) = \frac{2\delta}{\tilde{\Omega}_{\rm DE}} \frac{S(z)}{S(0)}, \tag{4.5}$$

$$S(z) = \frac{1}{2}\left[1 - \tanh\left(\frac{z - z_{\rm t}}{\Delta z}\right)\right], \tag{4.6}$$

where $\tilde{\rho}_{\rm DE}$ and $\tilde{\Omega}_{\rm DE}$ are the dark energy density and density parameter in a standard ΛCDM model. In this model, the dark energy density suddenly increases at redshift $z_{\rm t}$ as compared to its ΛCDM value by a fractional factor of 2δ, with Δz parameterizing the duration of the transition. As a result, this model boosts the $z = 0$ Hubble rate according to

$$H_0^2 = (1 + 2\delta)\tilde{H}_0^2, \tag{4.7}$$

where the tilde indicates the original ΛCDM value.

The critical feature of this model is that when $z \gg z_t$, it is indistinguishable from the ΛCDM model. In order to achieve a positive value of δ, the equation of state must be allowed to enter the phantom regime of $w < -1$, which can make a physical implementation of such a phenomenological model difficult. With its sudden late-time transition, this scenario nevertheless achieves the desired result of 'hiding' the reduced distance to the CMB last-scattering surface that usually results from increasing H_0. Indeed, using CMB and BAO data in conjunction with a Gaussian H_0 prior (based on the results of ref. [237]), ref. [88] showed that such model could achieve $H_0 = 72.5 \pm 1.85$ km/s/Mpc, hence apparently alleviating the tension.

JCAP06(2022)002

4.1.2 Taking into account the distance measurements: results

From the analysis quoted above, the LDE model considered here may seem like a promising way to resolve the Hubble-Lemaître Tension. However, such models are much less promising once the local distance ladder is properly accounted for [88]. As explained above, LDE-based solutions can increase the value of H_0 while causing a negligible fractional change in distance to the CMB last-scattering surface and thus to $\theta_\star$. However, the fractional change in distance to low-redshift SNe Ia from such late-time transition is, in general, not negligible. This can result in a poor fit to the actual distances, with the lowest redshift objects being the most affected. Therefore, LDE models, in general, are ideal examples of being too focused on modifying the value of H_0 itself while entirely missing the actual source of the tension (i.e. the distances).

The red line in figure 3 shows the distribution of intercepts values β (using the Cepheid calibration) for a LDE model fitted to Planck data and a Gaussian prior on H_0 from the R21 measurement. Recall that for no tension to exist, the intercept should be identically 0. In this case, the intercept value of the LDE model is $\beta = 0.073 \pm 0.04$, which is consistent with zero at less than two sigmas. While this seems to alleviate the tension between CMB and the Cepheid calibration, this solution is much less promising when looking at the individual distances to nearby supernovae. This is shown in figure 5 where we observe a clear offset at low redshifts ($z \lesssim 0.1$) between the actual distances to SNe Ia calibrated with Cepheids (blue points), and the corresponding distances predicted in the LDE model (red points) fitted with a Gaussian prior on H_0. The residual plot in the lower panel of figure 5 describes the difference in distance modulus required to bring the LDE-predicted SNe Ia distances into agreement with their measurements. We can further quantify this low-redshift distance tension by fitting the relationship between the predicted distance moduli μ and the measured $m - M_{\rm sn}$ values with a linear regression with a free slope. Recall that if this slope differs from unity, it would indicate a breakdown of the standard relationship between absolute luminosity and measured flux in an expanding Universe. Performing such fit, we find a slope of 0.983 ± 0.002, which differs from unity at 8.5 σ indicating a clear issue in this late-time dark energy model. The corresponding intercept is $\beta = 0.729 \pm 0.09$, which differs significantly from zero at several sigmas. Clearly, a late dark energy transition does nothing to address the root cause of the tension and can even make the global fit to cosmological data worse. In fact, comparing the LDE model fitted with a Gaussian prior on H_0 to the LDE model fitted with the *distanceladder* likelihood results in a $\Delta\chi^2 \sim 21$, demonstrating that the former provides a poorer fit to the distances than the latter. While these results are broadly consistent with those presented in ref. [88], our work clarifies why these models fail to properly resolve the tension: they are unable to fit the actual distance to low-redshift SNe Ia in the Hubble flow, as shown in figure 5.

Perhaps even more concerning is that using a Gaussian prior, in this case, could lead to spurious detection of new physics. As shown in figure 6 (see also table 2), the LDE model analyzed with Planck and BAO data in addition to a Gaussian H_0 prior leads to a significant detection ($> 3.5\sigma$) of a non-vanishing δ value, indicating a strong statistical preference for a late transition in the abundance of dark energy. However, when the actual calibrated distance measurements are taken into account as in our *distanceladder* likelihood, the value of δ becomes entirely consistent with zero, and no significant evidence for a late-time transition in the abundance of dark energy is observed. In this case, the failure of the Gaussian H_0 prior can be traced back to the breakdown of the standard cosmographic expansion of the luminosity distance to SNe Ia in the presence of a sharp transition in the Hubble rate at late times.

JCAP06(2022)002

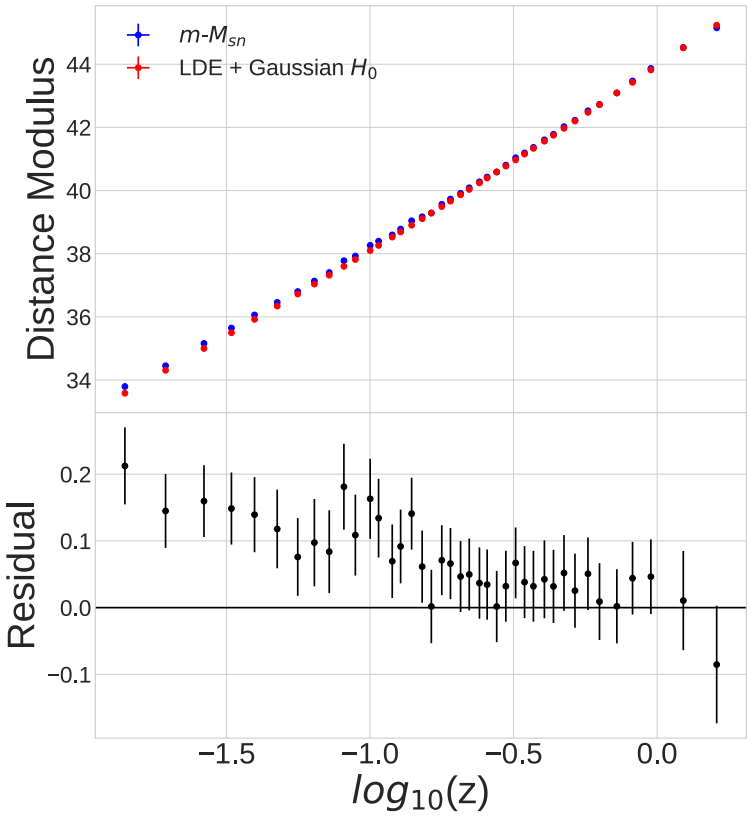

Figure 5. Comparison of the Cepheid-calibrated SNe Ia distance moduli from the Pantheon sample (blue) to the distance moduli predicted by a LDE model fitted with Planck CMB data, BAO data, and a Gaussian prior on H_0 (red). The residual difference between the measurements and the LDE predictions are shown in the bottom panel. The error bars on the blue and red points are smaller than the points themselves and are not easily seen. A systematic disagreement is seen between the Cepheid-calibrated distances and the LDE prediction with a Gaussian H_0 prior, especially at lower redshifts.

LDE	Distance Ladder H_0	Gaussian H_0
$100\theta_{\rm s}$	1.04200±0.00029	1.04170±0.00029
$\Omega_{\rm b}$	0.02246±0.00014	0.02247±0.00014
$\Omega_{\rm c}$	0.11867±0.00094	0.11890±0.00097
τ	0.0570±0.0076	0.0596±0.0073
$\ln(10^{10}{\rm A_s})$	3.050±0.015	3.052±0.015
$n_{\rm s}$	0.9694±0.0038	0.9689±0.0038
δ	0.022±0.022	0.091±0.048
H_0	69.74±1.28	73.78±2.15

Table 2. Table describing the mean and 68% confidence intervals of a MCMC in which the *distance-ladder* likelihood and the standard Gaussian likelihood on H_0 are used. Prior limited implies that the value is unconstrained within the prior. Δz and $z_{\rm t}$ are prior limited in all cases.

JCAP06(2022)002

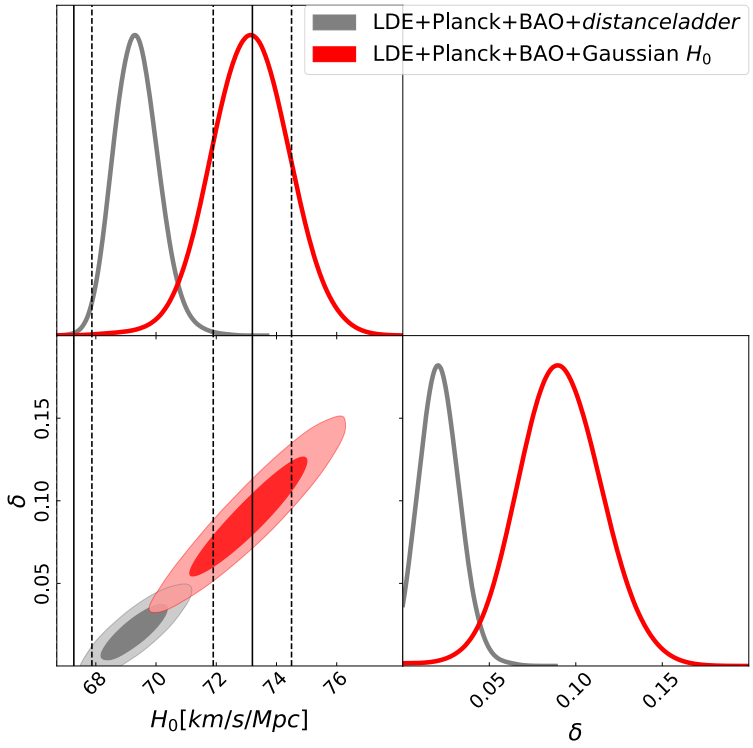

Figure 6. Posterior distributions involving a late-time dark energy model using the traditional Gaussian prior on H_0 indicated by red, and *distanceladder* likelihood package in grey. The solid black lines indicate the mean value from ref. [29] (left) and ref. [36] (right) with the dashed lines indicating the 1σ differences.

4.2 Discussion

The above section demonstrates that a Gaussian prior on H_0 can lead to a statistically significant detection of a dark energy transition at very late times. However, once the actual distances to SNe Ia are properly taken into account, such preference largely disappears. Figure 5 clearly illustrates why this is happening: the Gaussian prior on H_0 leads to distances to low-redshift SNe Ia that are too small compared with their actual measured values. Ultimately, this problem arises because the LDE models break the assumptions (in particular, the cosmographic expansion of the luminosity distance) that were used to infer H_0 from carefully calibrated distances to SNe Ia in the Hubble flow [34, 36]. This should serve as a cautionary tale when analyzing models that modify the Universe's expansion history at very late times. In general, we recommend that cosmological models that deviate significantly from ΛCDM at $z \lesssim 1$ should never be analyzed with a Gaussian prior on H_0. Instead, the calibrated distances to SNe Ia in the Hubble flow should directly be used in statistical analyses of such models. Our *distanceladder* likelihood package make such analyses straightforward.

Beyond the possible breakdown of the cosmographic expansion, another issue that has plagued many cosmological analyses using a Gaussian H_0 prior in conjunction with CMB data is the resulting ambiguity in the underlying absolute SNe Ia calibration. For example, R16 finds a value of $M_{\rm sn} = -19.214 \pm 0.037$. Imposing the corresponding Gaussian prior on H_0 implicitly assumes this $M_{\rm sn}$ value, which does not necessarily agree with the value of $M_{\rm sn}$ implied by the other likelihoods used. For instance, the Pantheon data set calibrated

JCAP06(2022)002

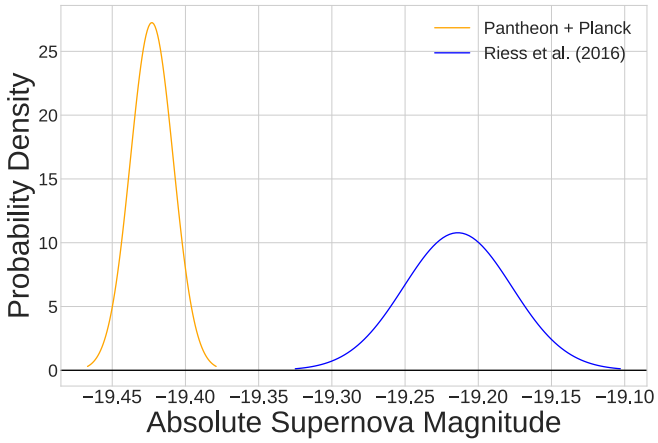

Figure 7. Comparison of the values of $M_{\rm sn}$ gotten by calibrating the Pantheon supernova data set with Planck data in ΛCDM with that obtained from the local distance ladder [34].

with Planck data finds a value of $M_{\rm sn} = -19.420 \pm 0.014$ in ΛCDM, which is statistically inconsistent with the above value as shown in figure 7. However, since most of the attention is focused on H_0 rather than the distances themselves, this underlying inconsistency is often missed in cosmological analyses. Of course, this $\beta \sim -0.2$ mag discrepancy between $M_{\rm sn}$ values *is* the root cause of the Hubble-Lemaître tension within ΛCDM. This point was recently emphasized in refs. [26, 27, 121, 238], and recent analyses of possible solutions to the tension have used $M_{\rm sn}$ instead of H_0 as their key parameters (see e.g. ref. [58]). However, as we have seen in figure 3, simply making the values of $M_{\rm sn}$ between the local and inverse distance ladders compatible (i.e. $\beta \sim 0$) is not necessarily sufficient to ensure a successful cosmological solution: the model must also fit the actual distances to SNe Ia.

5 Conclusion

An impressive amount of literature has been written on the Hubble-Lemaître tension, and it remains a real possibility that it could be the result of some missing pieces in our cosmological model. This impressive literature includes cosmological models that modify the cosmological expansion history at $z < 1$. Using a simple Gaussian prior distribution on H_0 to represent the entirety of the local distance ladder, some of these solutions can appear to be promising at relieving the tension. However, in using such a H_0 prior, the user implicitly assumes that the local distance ladder directly measures the Hubble expansion rate at $z = 0$. In reality, regardless of calibration choice, the local distance ladder actually measures distances to SNe Ia in the Hubble flow in the redshift range $z \gtrsim 0.02$. Therefore, to properly assess the effectiveness of cosmological models with modified late-time dynamics at relieving the Hubble-Lemaître tension, a simple Gaussian prior can not be used to represent the entire distance ladder. Instead, a likelihood that reconstructs the distance ladder and the distance measurements to the Hubble flow supernova is required for any model which proposes changes to the late-time Universe.

To aid in this, we have developed a likelihood package aptly named *distanceladder* which focuses on fitting the actual distances to SNe Ia, rather than simply fitting for H_0. The *distanceladder* likelihood uses the actual luminosity distance given by the proposed cosmological model and is therefore sensitive to any changes in cosmology presented. This

JCAP06(2022)002

publicly available numerical package allows the user to test the different assumptions made in analyzing the cosmological distance ladder. It is therefore much more flexible and insightful than simply specifying a prior on the absolute supernova magnitude. To demonstrate the effectiveness of the likelihood, we have used the example of a late-time transition in the abundance of dark energy to showcase how focusing purely on H_0 can lead to the spurious detection of new physics, and a false sense that the Hubble-Lemaître tension has been relieved. When the distances are correctly accounted for, such late-time dark energy transition are severely constrained in their ability to resolve the Hubble-Lemaître tension. This behaviour is not limited to only this late-time dark energy model but to any model which dramatically changes the late-time expansion history of the Universe as compared to ΛCDM. In general, the success of a cosmological model should be assessed by how well it can fit the actual distances to Hubble-flow objects (including supernovae, strong gravitational lenses, and gravitational waves standard sirens, among others), rather than whether it can reproduce a specific value of H_0. We encourage the observational cosmology community to make their actual distance measurements broadly available instead of emphasizing the derived Hubble constant values, which contain assumptions that might not be applicable to all cosmological scenarios.

Within the standard ΛCDM model, the Hubble-Lemaître tension between Cepheid-calibrated SNe Ia distances and Planck CMB data is now at the critical 5σ threshold [37]. Addressing this crucial cosmological problem requires the community to focus on the root cause of the tension — the distances to low-redshift Hubble-flow objects — rather than argue about which value of the Hubble constant might be the correct one.

Acknowledgments

This work was supported by the National Science Foundation (NSF) under grant AST-2008696. We would like to thank the UNM Center for Advanced Research Computing, supported in part by the NSF, for providing the research computing resources used in this work. Part of this work was performed at the Aspen Center for Physics, which is supported by NSF grant PHY-1607611.

A Distanceladder vs. Gaussian prior on $M_{\rm sn}$

We investigate the differences between using a Gaussian prior on $M_{\rm sn}$ along with the Pantheon likelihood and the *distanceladder* likelihood to represent the local measurement of H_0. Both methodologies utilize the distance modulus to compute the maximum likelihood statistics, but make subtle different assumptions in how the covariance matrix is handled. The Pantheon likelihood with Gaussian $M_{\rm sn}$ utilizes a pregenerated covariance matrix with the statistical error on the diagonal. The *distanceladder* covariance matrix is comprised of three parts. First, the square of the statistical error along the diagonal associated with measurements of the apparent magintude. Second, the square of the jacobian which originates from including the error in redshift given by

$$\delta J = \left(\frac{1+z}{H(z)} + \frac{d_{\rm L}}{1+z}\right)\delta z. \tag{A.1}$$

JCAP06(2022)002

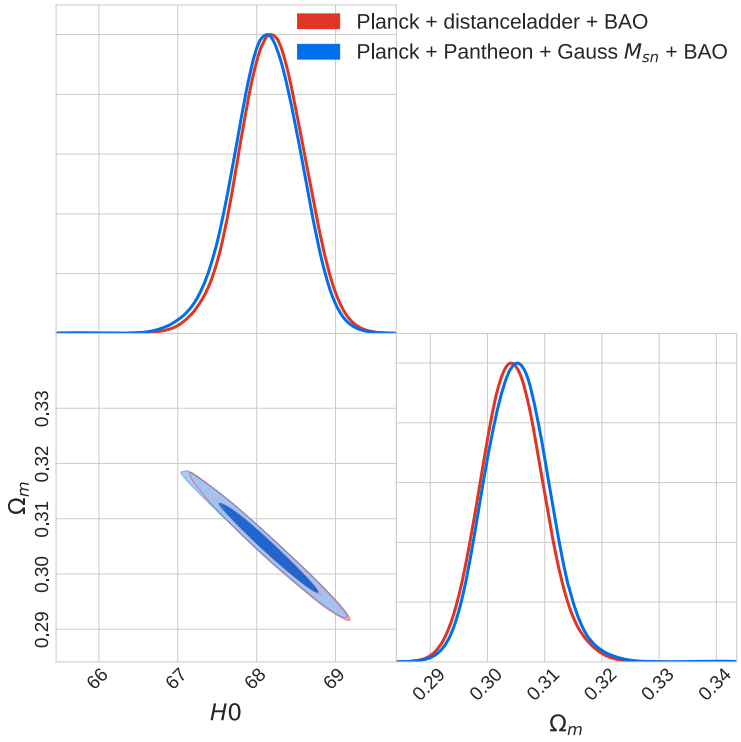

Figure 8. Posterior distributions comparing the results of using the *distanceladder* likelihood and the Pantheon likelihood with a gaussian prior placed on $M_{\rm sn}$ assuming a typical ΛCDM cosmology and including CMB and BAO data. The Planck data utilized are the TT, EE, TE modes and lensing. Here we see a slight difference between the *distanceladder* and the Pantheon likelihood with gaussian $M_{\rm sn}$, due to the different handling of the error on $M_{\rm sn}$.

Third, a dense matrix comprised of the square of the error associated with $M_{\rm sn}$. The final covariance matrix for the *distanceladder* is therefore given by

$$\begin{vmatrix} \delta m_{b,1}^2 + \delta J_1^2 + \delta M_{\rm sn}^2 & \delta M_{\rm sn}^2 & \dots & \delta M_{\rm sn}^2 \\ \delta M_{\rm sn}^2 & \delta m_{b,2}^2 + \delta J_2^2 + \delta M_{\rm sn}^2 & \dots & \delta M_{\rm sn}^2 \\ \vdots & \vdots & \ddots & \vdots \\ \delta M_{\rm sn}^2 & \delta M_{\rm sn}^2 & \dots & \delta m_{b,i}^2 + \delta J_i^2 + \delta M_{\rm sn}^2 \end{vmatrix}. \tag{A.2}$$

The results comparing the two methodologies are given in figure 8. We see a small difference between the two, primarily originating from the handling of the $\delta M_{\rm sn}$ error within *distanceladder*.

References

[1] H.S. Leavitt and E.C. Pickering, *Periods of 25 Variable Stars in the Small Magellanic Cloud*, *Harvard Obs. Circ.* **173** (1912) 1.

[2] V.M. Slipher, *Spectrographic Observations of Nebulae*, *Popular Astronomy* **23** (1915) 21.

[3] G. Lemaitre, *A Homogeneous Universe of Constant Mass and Growing Radius Accounting for the Radial Velocity of Extragalactic Nebulae*, *Annales Soc. Sci. Bruxelles A* **47** (1927) 49 [INSPIRE].

JCAP06(2022)002

[4] H.P. Robertson, *On relativistic cosmology*, *Philos. Mag.* **5** (1928) 835.

[5] E. Hubble, *A relation between distance and radial velocity among extra-galactic nebulae*, *Proc. Nat. Acad. Sci.* **15** (1929) 168 [INSPIRE].

[6] J. Evslin, A.A. Sen and Ruchika, *Price of shifting the Hubble constant*, *Phys. Rev. D* **97** (2018) 103511 [arXiv:1711.01051] [INSPIRE].

[7] K. Aylor, M. Joy, L. Knox, M. Millea, S. Raghunathan and W.L.K. Wu, *Sounds Discordant: Classical Distance Ladder & ΛCDM-based Determinations of the Cosmological Sound Horizon*, *Astrophys. J.* **874** (2019) 4 [arXiv:1811.00537] [INSPIRE].

[8] K. Jedamzik, L. Pogosian and G.-B. Zhao, *Why reducing the cosmic sound horizon alone can not fully resolve the Hubble tension*, *Commun. in Phys.* **4** (2021) 123 [arXiv:2010.04158] [INSPIRE].

[9] L. Pogosian, G.-B. Zhao and K. Jedamzik, *Recombination-independent determination of the sound horizon and the Hubble constant from BAO*, *Astrophys. J. Lett.* **904** (2020) L17 [arXiv:2009.08455] [INSPIRE].

[10] J.L. Bernal, T.L. Smith, K.K. Boddy and M. Kamionkowski, *Robustness of baryon acoustic oscillation constraints for early-Universe modifications of ΛCDM cosmology*, *Phys. Rev. D* **102** (2020) 123515 [arXiv:2004.07263] [INSPIRE].

[11] I. Semeniuk, *Comparison of parallaxes from eclipsing binaries method with hipparcos parallaxes*, *Acta Astron.* **50** (2000) 381 [astro-ph/0010133] [INSPIRE].

[12] GAIA collaboration, *The Gaia Mission*, *Astron. Astrophys.* **595** (2016) A1 [arXiv:1609.04153] [INSPIRE].

[13] C.A.L. Bailer-Jones, *Estimating distances from parallaxes*, *Publ. Astron. Soc. Pac.* **127** (2015) 994.

[14] B. Paczynski, *Detached eclipsing binaries as primary distance and age indicators*, astro-ph/9608094 [INSPIRE].

[15] A.Z. Bonanos et al., *The First DIRECT Distance Determination to a Detached Eclipsing Binary in M33*, *Astrophys. J.* **652** (2006) 313 [astro-ph/0606279] [INSPIRE].

[16] D. Graczyk, *Light curve solutions for bright detached eclipsing binaries in SMC: Absolute dimensions and distance indicators*, *Mon. Not. Roy. Astron. Soc.* **342** (2003) 1334 [astro-ph/0303550] [INSPIRE].

[17] M.J. Reid, D.W. Pesce and A.G. Riess, *An Improved Distance to NGC 4258 and its Implications for the Hubble Constant*, *Astrophys. J. Lett.* **886** (2019) L27 [arXiv:1908.05625] [INSPIRE].

[18] D. Pesce et al., *A geometric measurement of H_0 by the Megamaser Cosmology Project*, in *H_0 2020: Assessing Uncertainties in Hubble's Constant Across the Universe*, p. 20, (Oct., 2020), [DOI].

[19] S.A. Dzib et al., *A revised distance to iras 16293-2422 from vlba astrometry of associated water masers*, *Astron. Astrophys.* **614** (2018) A20.

[20] R.D. Blandford and R. Narayan, *Cosmological applications of gravitational lensing*, *Ann. Rev. Astron. Astrophys.* **30** (1992) 311 [INSPIRE].

[21] E. Eulaers and P. Magain, *Time delays for 11 gravitationally lensed quasars revisited*, *Astron. Astrophys.* **536** (2011) A44 [arXiv:1112.2609] [INSPIRE].

[22] N. Arendse, A. Agnello and R. Wojtak, *Low-redshift measurement of the sound horizon through gravitational time-delays*, *Astron. Astrophys.* **632** (2019) A91 [arXiv:1905.12000] [INSPIRE].

[23] J.L. Bernal, L. Verde and A.G. Riess, *The trouble with H_0*, *JCAP* **10** (2016) 019 [arXiv:1607.05617] [INSPIRE].

JCAP06(2022)002

[24] L. Verde, T. Treu and A.G. Riess, *Tensions between the Early and the Late Universe*, *Nature Astron.* **3** (2019) 891 [arXiv:1907.10625] [INSPIRE].

[25] L. Knox and M. Millea, *Hubble constant hunter's guide*, *Phys. Rev. D* **101** (2020) 043533 [arXiv:1908.03663] [INSPIRE].

[26] G. Efstathiou, *A Lockdown Perspective on the Hubble Tension (with comments from the SH0ES team)*, arXiv:2007.10716 [INSPIRE].

[27] G. Efstathiou, *To H0 or not to H0?*, *Mon. Not. Roy. Astron. Soc.* **505** (2021) 3866 [arXiv:2103.08723] [INSPIRE].

[28] P. Shah, P. Lemos and O. Lahav, *A buyer's guide to the Hubble constant*, *Astron. Astrophys. Rev.* **29** (2021) 9 [arXiv:2109.01161] [INSPIRE].

[29] PLANCK collaboration, *Planck 2018 results. VI. Cosmological parameters*, *Astron. Astrophys.* **641** (2020) A6 [*Erratum ibid.* **652** (2021) C4] [arXiv:1807.06209] [INSPIRE].

[30] ACT collaboration, *The Atacama Cosmology Telescope: DR4 Maps and Cosmological Parameters*, *JCAP* **12** (2020) 047 [arXiv:2007.07288] [INSPIRE].

[31] SPT-3G collaboration, *Measurements of the E-mode polarization and temperature-E-mode correlation of the CMB from SPT-3G 2018 data*, *Phys. Rev. D* **104** (2021) 022003 [arXiv:2101.01684] [INSPIRE].

[32] A.G. Riess et al., *A 3% Solution: Determination of the Hubble Constant with the Hubble Space Telescope and Wide Field Camera 3*, *Astrophys. J.* **730** (2011) 119 [*Erratum ibid.* **732** (2011) 129] [arXiv:1103.2976] [INSPIRE].

[33] W.L. Freedman et al., *Carnegie Hubble Program: A Mid-Infrared Calibration of the Hubble Constant*, *Astrophys. J.* **758** (2012) 24 [arXiv:1208.3281] [INSPIRE].

[34] A.G. Riess et al., *A 2.4% Determination of the Local Value of the Hubble Constant*, *Astrophys. J.* **826** (2016) 56 [arXiv:1604.01424] [INSPIRE].

[35] CSP collaboration, *The Carnegie Supernova Project: Absolute Calibration and the Hubble Constant*, *Astrophys. J.* **869** (2018) 56 [arXiv:1809.06381] [INSPIRE].

[36] A.G. Riess et al., *Cosmic Distances Calibrated to 1% Precision with Gaia EDR3 Parallaxes and Hubble Space Telescope Photometry of 75 Milky Way Cepheids Confirm Tension with ΛCDM*, *Astrophys. J. Lett.* **908** (2021) L6 [arXiv:2012.08534] [INSPIRE].

[37] A.G. Riess et al., *A Comprehensive Measurement of the Local Value of the Hubble Constant with 1 KM/s/Mpc Uncertainty from the Hubble Space Telescope and the SH0ES Team*, arXiv:2112.04510 [INSPIRE].

[38] R.L. Beaton et al., *The Carnegie-Chicago Hubble Program. I. An Independent Approach to the Extragalactic Distance Scale Using only Population II Distance Indicators*, *Astrophys. J.* **832** (2016) 210 [arXiv:1604.01788] [INSPIRE].

[39] D. Hatt et al., *The Carnegie-Chicago Hubble Program. II. The Distance to IC 1613: The Tip of the Red Giant Branch and RR Lyrae Period-luminosity Relations*, *Astrophys. J.* **845** (2017) 146 [arXiv:1703.06468] [INSPIRE].

[40] D. Hatt et al., *The Carnegie-Chicago Hubble Program. IV. The Distance to NGC 4424, NGC 4526, and NGC 4356 via the Tip of the Red Giant Branch*, *Astrophys. J.* **861** (2018) 104 [arXiv:1806.02900] [INSPIRE].

[41] D. Hatt et al., *The Carnegie-Chicago Hubble Program. V. The Distances to NGC 1448 and NGC 1316 via the Tip of the Red Giant Branch*, *Astrophys. J.* **866** (2018) 145 [arXiv:1809.01741] [INSPIRE].

[42] T.J. Hoyt et al., *The Carnegie Chicago Hubble program. VI. Tip of the red giant branch distances to M66 and M96 of the Leo I Group*, *Astrophys. J.* **882** (2019) 150.

JCAP06(2022)002

[43] R.L. Beaton et al., *The Carnegie-Chicago Hubble program. VII. The distance to m101 via the optical tip of the red giant branch method*, *Astrophys. J.* **885** (2019) 141.

[44] I.S. Jang et al., *The Carnegie-Chicago Hubble program. IX. Calibration of the tip of the red giant branch method in the Megamaser Host Galaxy, NGC 4258 (M106)*, *Astrophys. J.* **906** (2021) 125.

[45] T.J. Hoyt et al., *The carnegie chicago hubble program x: Tip of the red giant branch distances to ngc 5643 and ngc 1404*, *Astrophys. J.* **915** (2021) 34.

[46] W.L. Freedman et al., *The Carnegie-Chicago Hubble Program. VIII. An Independent Determination of the Hubble Constant Based on the Tip of the Red Giant Branch*, arXiv:1907.05922 [INSPIRE].

[47] W.L. Freedman et al., *Calibration of the Tip of the Red Giant Branch (TRGB)*, arXiv:2002.01550 [INSPIRE].

[48] W.L. Freedman, *Measurements of the Hubble Constant: Tensions in Perspective*, *Astrophys. J.* **919** (2021) 16 [arXiv:2106.15656] [INSPIRE].

[49] T. Treu and P.J. Marshall, *Time Delay Cosmography*, *Astron. Astrophys. Rev.* **24** (2016) 11 [arXiv:1605.05333] [INSPIRE].

[50] S.H. Suyu et al., *H0LiCOW — I. H0 Lenses in COSMOGRAIL's Wellspring: program overview*, *Mon. Not. Roy. Astron. Soc.* **468** (2017) 2590 [arXiv:1607.00017] [INSPIRE].

[51] S. Birrer et al., *H0LiCOW — IX. Cosmographic analysis of the doubly imaged quasar SDSS 1206+4332 and a new measurement of the Hubble constant*, *Mon. Not. Roy. Astron. Soc.* **484** (2019) 4726 [arXiv:1809.01274] [INSPIRE].

[52] K.C. Wong et al., *H0LiCOW — XIII. A 2.4 per cent measurement of H0 from lensed quasars: 5.3σ tension between early- and late-Universe probes*, *Mon. Not. Roy. Astron. Soc.* **498** (2020) 1420 [arXiv:1907.04869] [INSPIRE].

[53] S. Birrer et al., *TDCOSMO — IV. Hierarchical time-delay cosmography — joint inference of the Hubble constant and galaxy density profiles*, *Astron. Astrophys.* **643** (2020) A165 [arXiv:2007.02941] [INSPIRE].

[54] C. Krishnan, R. Mohayaee, E.O. Colgáin, M.M. Sheikh-Jabbari and L. Yin, *Does Hubble tension signal a breakdown in FLRW cosmology?*, *Class. Quant. Grav.* **38** (2021) 184001 [arXiv:2105.09790] [INSPIRE].

[55] C. Krishnan, R. Mohayaee, E.O. Colgáin, M.M. Sheikh-Jabbari and L. Yin, *Hints of FLRW breakdown from supernovae*, *Phys. Rev. D* **105** (2022) 063514 [arXiv:2106.02532] [INSPIRE].

[56] O. Luongo, M. Muccino, E.O. Colgáin, M.M. Sheikh-Jabbari and L. Yin, *Larger H0 values in the CMB dipole direction*, *Phys. Rev. D* **105** (2022) 103510 [arXiv:2108.13228] [INSPIRE].

[57] E. Di Valentino et al., *In the realm of the Hubble tension — a review of solutions*, *Class. Quant. Grav.* **38** (2021) 153001 [arXiv:2103.01183] [INSPIRE].

[58] N. Schöneberg, G. Franco Abellán, A. Pérez Sánchez, S.J. Witte, V. Poulin and J. Lesgourgues, *The H_0 Olympics: A fair ranking of proposed models*, arXiv:2107.10291 [INSPIRE].

[59] T. Karwal and M. Kamionkowski, *Dark energy at early times, the Hubble parameter, and the string axiverse*, *Phys. Rev. D* **94** (2016) 103523 [arXiv:1608.01309] [INSPIRE].

[60] V. Poulin, T.L. Smith, T. Karwal and M. Kamionkowski, *Early Dark Energy Can Resolve The Hubble Tension*, *Phys. Rev. Lett.* **122** (2019) 221301 [arXiv:1811.04083] [INSPIRE].

[61] T.L. Smith, V. Poulin and M.A. Amin, *Oscillating scalar fields and the Hubble tension: a resolution with novel signatures*, *Phys. Rev. D* **101** (2020) 063523 [arXiv:1908.06995] [INSPIRE].

JCAP06(2022)002

[62] T.L. Smith, V. Poulin, J.L. Bernal, K.K. Boddy, M. Kamionkowski and R. Murgia, *Early dark energy is not excluded by current large-scale structure data*, *Phys. Rev. D* **103** (2021) 123542 [arXiv:2009.10740] [INSPIRE].

[63] V. Poulin, T.L. Smith and A. Bartlett, *Dark energy at early times and ACT data: A larger Hubble constant without late-time priors*, *Phys. Rev. D* **104** (2021) 123550 [arXiv:2109.06229] [INSPIRE].

[64] P. Agrawal, F.-Y. Cyr-Racine, D. Pinner and L. Randall, *Rock 'n' Roll Solutions to the Hubble Tension*, arXiv:1904.01016 [INSPIRE].

[65] F.-Y. Cyr-Racine, F. Ge and L. Knox, *A Symmetry of Cosmological Observables, and a High Hubble Constant as an Indicator of a Mirror World Dark Sector*, arXiv:2107.13000 [INSPIRE].

[66] R. Murgia, G.F. Abellán and V. Poulin, *Early dark energy resolution to the Hubble tension in light of weak lensing surveys and lensing anomalies*, *Phys. Rev. D* **103** (2021) 063502 [arXiv:2009.10733] [INSPIRE].

[67] C. Krishnan, E.O. Colgáin, Ruchika, A.A. Sen, M.M. Sheikh-Jabbari and T. Yang, *Is there an early Universe solution to Hubble tension?*, *Phys. Rev. D* **102** (2020) 103525 [arXiv:2002.06044] [INSPIRE].

[68] N. Blinov and G. Marques-Tavares, *Interacting radiation after Planck and its implications for the Hubble Tension*, *JCAP* **09** (2020) 029 [arXiv:2003.08387] [INSPIRE].

[69] N. Blinov, C. Keith and D. Hooper, *Warm Decaying Dark Matter and the Hubble Tension*, *JCAP* **06** (2020) 005 [arXiv:2004.06114] [INSPIRE].

[70] F. Niedermann and M.S. Sloth, *Resolving the Hubble tension with new early dark energy*, *Phys. Rev. D* **102** (2020) 063527 [arXiv:2006.06686] [INSPIRE].

[71] G. Choi, T.T. Yanagida and N. Yokozaki, *A model of interacting dark matter and dark radiation for H_0 and σ_8 tensions*, *JHEP* **01** (2021) 127 [arXiv:2010.06892] [INSPIRE].

[72] C.D. Kreisch, F.-Y. Cyr-Racine and O. Doré, *Neutrino puzzle: Anomalies, interactions, and cosmological tensions*, *Phys. Rev. D* **101** (2020) 123505 [arXiv:1902.00534] [INSPIRE].

[73] T. Brinckmann, J.H. Chang and M. LoVerde, *Self-interacting neutrinos, the Hubble parameter tension, and the cosmic microwave background*, *Phys. Rev. D* **104** (2021) 063523 [arXiv:2012.11830] [INSPIRE].

[74] A. Das and S. Ghosh, *Flavor-specific interaction favors strong neutrino self-coupling in the early universe*, *JCAP* **07** (2021) 038 [arXiv:2011.12315] [INSPIRE].

[75] A. Mazumdar, S. Mohanty and P. Parashari, *Flavour specific neutrino self-interaction: H_0 tension and IceCube*, arXiv:2011.13685 [INSPIRE].

[76] D. Aloni, A. Berlin, M. Joseph, M. Schmaltz and N. Weiner, *A Step in Understanding the Hubble Tension*, arXiv:2111.00014 [INSPIRE].

[77] J. Sakstein and M. Trodden, *Early Dark Energy from Massive Neutrinos as a Natural Resolution of the Hubble Tension*, *Phys. Rev. Lett.* **124** (2020) 161301 [arXiv:1911.11760] [INSPIRE].

[78] M. Carrillo González, Q. Liang, J. Sakstein and M. Trodden, *Neutrino-Assisted Early Dark Energy: Theory and Cosmology*, *JCAP* **04** (2021) 063 [arXiv:2011.09895] [INSPIRE].

[79] K. Jedamzik and L. Pogosian, *Relieving the Hubble tension with primordial magnetic fields*, *Phys. Rev. Lett.* **125** (2020) 181302 [arXiv:2004.09487] [INSPIRE].

[80] M. Rashkovetskyi, J.B. Muñoz, D.J. Eisenstein and C. Dvorkin, *Small-scale clumping at recombination and the Hubble tension*, *Phys. Rev. D* **104** (2021) 103517 [arXiv:2108.02747] [INSPIRE].

JCAP06(2022)002

[81] T. Sekiguchi and T. Takahashi, *Early recombination as a solution to the H_0 tension*, *Phys. Rev. D* **103** (2021) 083507 [arXiv:2007.03381] [INSPIRE].

[82] L. Hart and J. Chluba, *Updated fundamental constant constraints from Planck 2018 data and possible relations to the Hubble tension*, *Mon. Not. Roy. Astron. Soc.* **493** (2020) 3255 [arXiv:1912.03986] [INSPIRE].

[83] M.J. Mortonson, W. Hu and D. Huterer, *Hiding dark energy transitions at low redshift*, *Phys. Rev. D* **80** (2009) 067301 [arXiv:0908.1408] [INSPIRE].

[84] S. Dhawan, D. Brout, D. Scolnic, A. Goobar, A.G. Riess and V. Miranda, *Cosmological Model Insensitivity of Local H_0 from the Cepheid Distance Ladder*, *Astrophys. J.* **894** (2020) 54 [arXiv:2001.09260] [INSPIRE].

[85] H.K. Jassal, J.S. Bagla and T. Padmanabhan, *Observational constraints on low redshift evolution of dark energy: How consistent are different observations?*, *Phys. Rev. D* **72** (2005) 103503 [astro-ph/0506748] [INSPIRE].

[86] R.R. Caldwell, M. Kamionkowski and N.N. Weinberg, *Phantom energy and cosmic doomsday*, *Phys. Rev. Lett.* **91** (2003) 071301 [astro-ph/0302506] [INSPIRE].

[87] E. Di Valentino, A. Mukherjee and A.A. Sen, *Dark Energy with Phantom Crossing and the H_0 Tension*, *Entropy* **23** (2021) 404 [arXiv:2005.12587] [INSPIRE].

[88] G. Benevento, W. Hu and M. Raveri, *Can Late Dark Energy Transitions Raise the Hubble constant?*, *Phys. Rev. D* **101** (2020) 103517 [arXiv:2002.11707] [INSPIRE].

[89] G. Alestas, L. Kazantzidis and L. Perivolaropoulos, *$w - M$ phantom transition at $z_t < 0.1$ as a resolution of the Hubble tension*, *Phys. Rev. D* **103** (2021) 083517 [arXiv:2012.13932] [INSPIRE].

[90] R.E. Keeley, S. Joudaki, M. Kaplinghat and D. Kirkby, *Implications of a transition in the dark energy equation of state for the H_0 and σ_8 tensions*, *JCAP* **12** (2019) 035 [arXiv:1905.10198] [INSPIRE].

[91] K. Dutta, Ruchika, A. Roy, A.A. Sen and M.M. Sheikh-Jabbari, *Beyond ΛCDM with low and high redshift data: implications for dark energy*, *Gen. Rel. Grav.* **52** (2020) 15 [arXiv:1808.06623] [INSPIRE].

[92] G. Alestas et al., *Late-transition versus smooth H(z)-deformation models for the resolution of the Hubble crisis*, *Phys. Rev. D* **105** (2022) 063538 [arXiv:2110.04336] [INSPIRE].

[93] S.J. Clark, K. Vattis and S.M. Koushiappas, *Cosmological constraints on late-universe decaying dark matter as a solution to the H_0 tension*, *Phys. Rev. D* **103** (2021) 043014 [arXiv:2006.03678] [INSPIRE].

[94] M. Braglia et al., *Larger value for H_0 by an evolving gravitational constant*, *Phys. Rev. D* **102** (2020) 023529 [arXiv:2004.11161] [INSPIRE].

[95] M. Ballardini, M. Braglia, F. Finelli, D. Paoletti, A.A. Starobinsky and C. Umiltà, *Scalar-tensor theories of gravity, neutrino physics, and the H_0 tension*, *JCAP* **10** (2020) 044 [arXiv:2004.14349] [INSPIRE].

[96] T. Karwal, M. Raveri, B. Jain, J. Khoury and M. Trodden, *Chameleon early dark energy and the Hubble tension*, *Phys. Rev. D* **105** (2022) 063535 [arXiv:2106.13290] [INSPIRE].

[97] R.C. Nunes and E. Di Valentino, *Dark sector interaction and the supernova absolute magnitude tension*, *Phys. Rev. D* **104** (2021) 063529 [arXiv:2107.09151] [INSPIRE].

[98] W. Yang, S. Pan, E. Di Valentino, R.C. Nunes, S. Vagnozzi and D.F. Mota, *Tale of stable interacting dark energy, observational signatures, and the H_0 tension*, *JCAP* **09** (2018) 019 [arXiv:1805.08252] [INSPIRE].

JCAP06(2022)002

[99] W. Yang, S. Pan, E. Di Valentino, E.N. Saridakis and S. Chakraborty, *Observational constraints on one-parameter dynamical dark-energy parametrizations and the H_0 tension*, *Phys. Rev. D* **99** (2019) 043543 [arXiv:1810.05141] [INSPIRE].

[100] W. Yang, A. Mukherjee, E. Di Valentino and S. Pan, *Interacting dark energy with time varying equation of state and the H_0 tension*, *Phys. Rev. D* **98** (2018) 123527 [arXiv:1809.06883] [INSPIRE].

[101] W. Yang, E. Di Valentino, S. Pan and O. Mena, *Emergent Dark Energy, neutrinos and cosmological tensions*, *Phys. Dark Univ.* **31** (2021) 100762 [arXiv:2007.02927] [INSPIRE].

[102] W. Yang, E. Di Valentino, O. Mena, S. Pan and R.C. Nunes, *All-inclusive interacting dark sector cosmologies*, *Phys. Rev. D* **101** (2020) 083509 [arXiv:2001.10852] [INSPIRE].

[103] W. Yang, E. Di Valentino, S. Pan, Y. Wu and J. Lu, *Dynamical dark energy after Planck CMB final release and H_0 tension*, *Mon. Not. Roy. Astron. Soc.* **501** (2021) 5845 [arXiv:2101.02168] [INSPIRE].

[104] W. Yang, E. Di Valentino, S. Pan, A. Shafieloo and X. Li, *Generalized emergent dark energy model and the Hubble constant tension*, *Phys. Rev. D* **104** (2021) 063521 [arXiv:2103.03815] [INSPIRE].

[105] W. Yang, S. Pan, E. Di Valentino, O. Mena and A. Melchiorri, *2021-H0 odyssey: closed, phantom and interacting dark energy cosmologies*, *JCAP* **10** (2021) 008 [arXiv:2101.03129] [INSPIRE].

[106] E. Di Valentino, A. Melchiorri and J. Silk, *Reconciling Planck with the local value of H_0 in extended parameter space*, *Phys. Lett. B* **761** (2016) 242 [arXiv:1606.00634] [INSPIRE].

[107] E. Di Valentino, E.V. Linder and A. Melchiorri, *Vacuum phase transition solves the H_0 tension*, *Phys. Rev. D* **97** (2018) 043528 [arXiv:1710.02153] [INSPIRE].

[108] E. Di Valentino, R.Z. Ferreira, L. Visinelli and U. Danielsson, *Late time transitions in the quintessence field and the H_0 tension*, *Phys. Dark Univ.* **26** (2019) 100385 [arXiv:1906.11255] [INSPIRE].

[109] E. Di Valentino, A. Melchiorri, O. Mena and S. Vagnozzi, *Interacting dark energy in the early 2020s: A promising solution to the H_0 and cosmic shear tensions*, *Phys. Dark Univ.* **30** (2020) 100666 [arXiv:1908.04281] [INSPIRE].

[110] E. Di Valentino, A. Melchiorri, O. Mena and S. Vagnozzi, *Nonminimal dark sector physics and cosmological tensions*, *Phys. Rev. D* **101** (2020) 063502 [arXiv:1910.09853] [INSPIRE].

[111] E. Di Valentino, E.V. Linder and A. Melchiorri, *H_0 ex machina: Vacuum metamorphosis and beyond H_0*, *Phys. Dark Univ.* **30** (2020) 100733 [arXiv:2006.16291] [INSPIRE].

[112] E. Di Valentino, A. Melchiorri, O. Mena, S. Pan and W. Yang, *Interacting Dark Energy in a closed universe*, *Mon. Not. Roy. Astron. Soc.* **502** (2021) L23 [arXiv:2011.00283] [INSPIRE].

[113] E. Di Valentino and O. Mena, *A fake Interacting Dark Energy detection?*, *Mon. Not. Roy. Astron. Soc.* **500** (2020) L22 [arXiv:2009.12620] [INSPIRE].

[114] E. Di Valentino, *A combined analysis of the H_0 late time direct measurements and the impact on the Dark Energy sector*, *Mon. Not. Roy. Astron. Soc.* **502** (2021) 2065 [arXiv:2011.00246] [INSPIRE].

[115] E. Di Valentino, S. Gariazzo, C. Giunti, O. Mena, S. Pan and W. Yang, *Minimal dark energy: Key to sterile neutrino and Hubble constant tensions?*, *Phys. Rev. D* **105** (2022) 103511 [arXiv:2110.03990] [INSPIRE].

[116] E. Di Valentino, S. Pan, W. Yang and L.A. Anchordoqui, *Touch of neutrinos on the vacuum metamorphosis: Is the H_0 solution back?*, *Phys. Rev. D* **103** (2021) 123527 [arXiv:2102.05641] [INSPIRE].

JCAP06(2022)002

[117] W. Lin, K.J. Mack and L. Hou, *Investigating the Hubble Constant Tension — Two Numbers in the Standard Cosmological Model*, *Astrophys. J. Lett.* **904** (2020) L22 [arXiv:1910.02978] [INSPIRE].

[118] W. Lin, X. Chen and K.J. Mack, *Early-Universe-Physics Insensitive and Uncalibrated Cosmic Standards: Constraints on $\Omega_{\rm m}$ and Implications for the Hubble Tension*, *Astrophys. J.* **920** (2021) 159 [arXiv:2102.05701] [INSPIRE].

[119] C. Garcia-Quintero, M. Ishak, L. Fox and W. Lin, *Cosmological discordances. III. More on measure properties, large-scale-structure constraints, the Hubble constant and Planck data*, *Phys. Rev. D* **100** (2019) 123538 [arXiv:1910.01608] [INSPIRE].

[120] S. Pan, W. Yang, E. Di Valentino, A. Shafieloo and S. Chakraborty, *Reconciling H_0 tension in a six parameter space?*, *JCAP* **06** (2020) 062 [arXiv:1907.12551] [INSPIRE].

[121] D. Camarena and V. Marra, *On the use of the local prior on the absolute magnitude of Type Ia supernovae in cosmological inference*, *Mon. Not. Roy. Astron. Soc.* **504** (2021) 5164 [arXiv:2101.08641] [INSPIRE].

[122] R. Jimenez and A. Loeb, *Constraining cosmological parameters based on relative galaxy ages*, *Astrophys. J.* **573** (2002) 37 [astro-ph/0106145] [INSPIRE].

[123] D. Stern, R. Jimenez, L. Verde, M. Kamionkowski and S.A. Stanford, *Cosmic Chronometers: Constraining the Equation of State of Dark Energy. I: H(z) Measurements*, *JCAP* **02** (2010) 008 [arXiv:0907.3149] [INSPIRE].

[124] S.M. Crawford, A.L. Ratsimbazafy, C.M. Cress, E.A. Olivier, S.-L. Blyth and K.J. van der Heyden, *Luminous Red Galaxies in Simulations: Cosmic Chronometers?*, *Mon. Not. Roy. Astron. Soc.* **406** (2010) 2569 [arXiv:1004.2378] [INSPIRE].

[125] F. Melia and R.S. Maier, *Cosmic Chronometers in the $R_h = ct$ Universe*, *Mon. Not. Roy. Astron. Soc.* **432** (2013) 2669 [arXiv:1304.1802] [INSPIRE].

[126] J.-J. Wei, F. Melia and X.-F. Wu, *Impact of a Locally Measured H_0 on the Interpretation of Cosmic-chronometer Data*, *Astrophys. J.* **835** (2017) 270 [arXiv:1612.08491] [INSPIRE].

[127] C.-Z. Ruan, F. Melia, Y. Chen and T.-J. Zhang, *Using spatial curvature with HII galaxies and cosmic chronometers to explore the tension in H_0*, *Astrophys. J.* **881** (2019) 137 [arXiv:1901.06626] [INSPIRE].

[128] N. Borghi, M. Moresco and A. Cimatti, *Toward a Better Understanding of Cosmic Chronometers: A New Measurement of H_z at $z \sim 0.7$*, *Astrophys. J. Lett.* **928** (2022) L4 [arXiv:2110.04304] [INSPIRE].

[129] D.E. Holz and S.A. Hughes, *Using gravitational-wave standard sirens*, *Astrophys. J.* **629** (2005) 15 [astro-ph/0504616] [INSPIRE].

[130] A. Nishizawa, K. Yagi, A. Taruya and T. Tanaka, *Gravitational-wave standard siren without redshift identification*, *J. Phys. Conf. Ser.* **363** (2012) 012052 [arXiv:1204.2877] [INSPIRE].

[131] LIGO Scientific and Virgo collaborations, *Observation of Gravitational Waves from a Binary Black Hole Merger*, *Phys. Rev. Lett.* **116** (2016) 061102 [arXiv:1602.03837] [INSPIRE].

[132] LIGO Scientific, Virgo, 1M2H, Dark Energy Camera GW-E, DES, DLT40, Las Cumbres Observatory, VINROUGE and MASTER collaborations, *A gravitational-wave standard siren measurement of the Hubble constant*, *Nature* **551** (2017) 85 [arXiv:1710.05835] [INSPIRE].

[133] E. Belgacem, Y. Dirian, S. Foffa and M. Maggiore, *Modified gravitational-wave propagation and standard sirens*, *Phys. Rev. D* **98** (2018) 023510 [arXiv:1805.08731] [INSPIRE].

[134] J.P. Blakeslee, E.A. Ajhar and J.L. Tonry, *Distances from surface brightness fluctuations*, *Astrophys. Space Sci. Libr.* **237** (1999) 181 [astro-ph/9807124] [INSPIRE].

JCAP06(2022)002

[135] M.C. Liu and J.R. Graham, *Infrared surface brightness fluctuations of the coma elliptical ngc 4874 and the value of the Hubble constant*, *Astrophys. J. Lett.* **557** (2001) L31 [astro-ph/0107471] [INSPIRE].

[136] N. Khetan et al., *A new measurement of the Hubble constant using Type Ia supernovae calibrated with surface brightness fluctuations*, *Astron. Astrophys.* **647** (2021) A72 [arXiv:2008.07754] [INSPIRE].

[137] J. Blakeslee, *Surface Brightness Fluctuations as Primary and Secondary Distance Indicators*, *Astrophys. Space Sci.* **341** (2012) 179 [arXiv:1202.0581] [INSPIRE].

[138] A. Fritz, *Distance Measurements and Stellar Population Properties via Surface Brightness Fluctuations*, *Publ. Astron. Soc. Austral.* **29** (2012) 489 [arXiv:1205.1498] [INSPIRE].

[139] J.B. Jensen, J.L. Tonry and G.A. Luppino, *Measuring distances using infrared surface brightness fluctuations*, *Astrophys. J.* **505** (1998) 111 [astro-ph/9804169] [INSPIRE].

[140] R. Giovanelli, *The i-band Tully-Fisher relation and the Hubble constant*, astro-ph/9610116 [INSPIRE].

[141] S. Sakai et al., *The Hubble Space Telescope Key Project on the Extragalactic Distance Scale. 24. The Calibration of Tully-Fisher relations and the value of the Hubble Constant*, *Astrophys. J.* **529** (2000) 698 [astro-ph/9909269] [INSPIRE].

[142] Y. Tutui, Y. Sofue, M. Honma, T. Ichikawa and K. Wakamatsu, *Hubble constant at intermediate redshift using the co-line Tully-Fisher relation*, *Publ. Astron. Soc. Jap.* **53** (2001) 701 [astro-ph/0108462] [INSPIRE].

[143] N. Bonhomme, H.M. Courtois and R.B. Tully, *Derivation of Distances with the Tully-Fisher Relation: The Antlia Cluster*, arXiv:0806.1140 [INSPIRE].

[144] Y. Sofue et al., *Distance measurement of galaxies to redshift* ~ 0.1 *using the CO-line Tully-Fisher relation*, *Publ. Astron. Soc. Jap.* **48** (1996) 657 [astro-ph/9607024] [INSPIRE].

[145] D.G. Russell, *The Ks-band Tully-Fisher Relation — A Determination of the Hubble Parameter from 218 ScI Galaxies and 16 Galaxy Clusters*, *J. Astrophys. Astron.* **30** (2009) 93 [arXiv:0812.1288] [INSPIRE].

[146] E. Kourkchi et al., *Cosmicflows-4: The catalog of* $\sim 10,000$ *Tully-Fisher distances*, *Astrophys. J.* **902** (2020) 145.

[147] E.E.E. Gall et al., *An updated Type II supernova Hubble diagram*, *Astron. Astrophys.* **611** (2018) A25 [arXiv:1705.10806] [INSPIRE].

[148] S. Blinnikov, M. Potashov, P. Baklanov and A. Dolgov, *Direct Determination of Hubble Parameter Using Type IIn Supernovae*, *Pisma Zh. Eksp. Teor. Fiz.* **96** (2012) 167 [arXiv:1207.6914] [INSPIRE].

[149] T. de Jaeger, B.E. Stahl, W. Zheng, A.V. Filippenko, A.G. Riess and L. Galbany, *A measurement of the Hubble constant from Type II supernovae*, *Mon. Not. Roy. Astron. Soc.* **496** (2020) 3402 [arXiv:2006.03412] [INSPIRE].

[150] M. Hamuy, *The Standard Candle Method for Type II Supernovae and the Hubble Constan*, *Springer Proc. Phys.* **99** (2005) 535 [astro-ph/0309122] [INSPIRE].

[151] SNLS collaboration, *Towards a Cosmological Hubble Diagram for Type II-P Supernovae*, *Astrophys. J.* **645** (2006) 841 [astro-ph/0603535] [INSPIRE].

[152] T. de Jaeger et al., *A Type II Supernova Hubble diagram from the CSP-I, SDSS-II, and SNLS surveys*, *Astrophys. J.* **835** (2017) 166 [arXiv:1612.05636] [INSPIRE].

[153] R. Chavez et al., *Determining the Hubble constant using Giant extragalactic HII regions and HII galaxies*, *Mon. Not. Roy. Astron. Soc.* **425** (2012) 56 [arXiv:1203.6222] [INSPIRE].

JCAP06(2022)002

[154] K. Leaf and F. Melia, *A two-point diagnostic for the H ii galaxy Hubble diagram*, *Mon. Not. Roy. Astron. Soc.* **474** (2018) 4507 [arXiv:1711.10793] [INSPIRE].

[155] M.K. Yennapureddy and F. Melia, *Reconstruction of the HII Galaxy Hubble Diagram using Gaussian Processes*, *JCAP* **11** (2017) 029 [arXiv:1711.03454] [INSPIRE].

[156] J.-J. Wei, X.-F. Wu and F. Melia, *The HII Galaxy Hubble Diagram Strongly Favors $R_h = ct$ over ΛCDM*, *Mon. Not. Roy. Astron. Soc.* **463** (2016) 1144 [arXiv:1608.02070] [INSPIRE].

[157] S. Casertano et al., *Parallax of Galactic Cepheids from Spatially Scanning the Wide Field Camera 3 on the Hubble Space Telescope: The Case of SS Canis Majoris*, *Astrophys. J.* **825** (2016) 11 [arXiv:1512.09371] [INSPIRE].

[158] F. van Leeuwen, M.W. Feast, P.A. Whitelock and C.D. Laney, *Cepheid Parallaxes and the Hubble Constant*, *Mon. Not. Roy. Astron. Soc.* **379** (2007) 723 [arXiv:0705.1592] [INSPIRE].

[159] A.G. Riess et al., *New Parallaxes of Galactic Cepheids from Spatially Scanning the Hubble Space Telescope: Implications for the Hubble Constant*, *Astrophys. J.* **855** (2018) 136 [arXiv:1801.01120] [INSPIRE].

[160] B.F. Madore and W.L. Freedman, *Hipparcos parallaxes and the Cepheid distance scale*, *Astrophys. J.* **492** (1998) 110 [astro-ph/9707091] [INSPIRE].

[161] C.A.L. Bailer-Jones, J. Rybizki, M. Fouesneau, G. Mantelet and R. Andrae, *Estimating distance from parallaxes. IV. Distances to 1.33 billion stars in gaia data release 2*, *Astron. J.* **156** (2018) 58.

[162] M.A.C. Perryman et al., *The Hipparcos catalogue*, *Astron. Astrophys.* **323** (1997) L49 [INSPIRE].

[163] C. Fabricius et al., *Gaia early data release 3*, *Astron. Astrophys.* **649** (2021) A5.

[164] G. Pietrzyński et al., *An eclipsing binary distance to the Large Magellanic Cloud accurate to 2 per cent*, *Nature* **495** (2013) 76 [arXiv:1303.2063] [INSPIRE].

[165] F. Vilardell, I. Ribas, C. Jordi, E.L. Fitzpatrick and E.F. Guinan, *The distance to the Andromeda Galaxy from eclipsing binaries*, *Astron. Astrophys.* **509** (2010) A70 [arXiv:0911.3391] [INSPIRE].

[166] J. Southworth, *DEBCat: A Catalog of Detached Eclipsing Binary Stars*, in *Living Together: Planets, Host Stars and Binaries*, S.M. Rucinski, G. Torres and M. Zejda, eds., vol. 496 of *ASP Conf. Ser.*, p. 164, July, 2015 [arXiv:1411.1219].

[167] I. Semeniuk, *Detached eclipsing binaries for parallax measurement*, astro-ph/0103511 [INSPIRE].

[168] B.K. Wiggins, V. Migenes and J.M. Smidt, *The hydroxyl-water megamaser connection. i. water emission toward oh megamaser hosts*, *Astrophys. J.* **816** (2016) 55.

[169] A. Tarchi, *AGN and Megamasers*, *IAU Symp.* **287** (2012) 323 [arXiv:1205.3623] [INSPIRE].

[170] Y.M. Pihlstrom, W.A. Baan, J. Darling and H.R. Klockner, *High-resolution imaging of the OH megamaser emission in IRAS 12032+1707 and IRAS 14070+0525*, *Astrophys. J.* **618** (2005) 705 [astro-ph/0410134] [INSPIRE].

[171] F. Gao et al., *The Megamaser Cosmology Project VIII. A Geometric Distance to NGC 5765b*, *Astrophys. J.* **817** (2016) 128 [arXiv:1511.08311] [INSPIRE].

[172] C. Kuo et al., *The Megamaser Cosmology Project. V. An Angular Diameter Distance to NGC 6264 at 140 Mpc*, *Astrophys. J.* **767** (2013) 155 [arXiv:1207.7273] [INSPIRE].

[173] E. Pitjeva and E. Standish, *Proposals for the masses of the three largest asteroids, the moon-earth mass ratio and the astronomical unit*, *Celest. Mech. Dyn. Astron.* **103** (2009) 365.

[174] B. Luzum et al., *The IAU 2009 system of astronomical constants: the report of the IAU working group on numerical standards for Fundamental Astronomy*, *Celest. Mech. Dyn. Astron.* **110** (2011) 293.

[175] F. van Leeuwen et al., *Gaiadata release 1*, *Astron. Astrophys.* **599** (2017) A32.

[176] X. Luri et al., *Gaia data release 2*, *Astron. Astrophys.* **616** (2018) A9.

[177] F. Torra et al., *Gaia early data release 3*, *Astron. Astrophys.* **649** (2021) A10.

[178] G. Pietrzyński et al., *A distance to the Large Magellanic Cloud that is precise to one per cent*, *Nature* **567** (2019) 200 [arXiv:1903.08096].

[179] J. Southworth, B. Smalley, P.F.L. Maxted, A. Claret and P.B. Etzel, *Absolute dimensions of detached eclipsing binaries. 1. The Metallic-lined system WW Aurigae*, *Mon. Not. Roy. Astron. Soc.* **363** (2005) 529 [astro-ph/0507629] [INSPIRE].

[180] B.A. Remple, G.C. Angelou and A. Weiss, *Determining fundamental parameters of detached double-lined eclipsing binary systems via a statistically robust machine learning method*, *Mon. Not. Roy. Astron. Soc.* **507** (2021) 1795.

[181] I.B. Thompson et al., *Cluster AgeS Experiment: The Age and Distance of the Globular Cluster ω Centauri Determined from Observations of the Eclipsing Binary OGLEGC 17*, *Astron. J.* **121** (2001) 3089 [astro-ph/0012493] [INSPIRE].

[182] A. Salsi et al., *Progress on the calibration of surface brightness-color relations for early- and late-type stars*, *Astron. Astrophys.* **652** (2021) A26 [arXiv:2106.01073].

[183] M.J. Reid, J.M. Moran and C.R. Gwinn, *Masers and the Cosmic Distance Scale (invited)*, in *The Impact of VLBI on Astrophysics and Geophysics*, M.J. Reid and J.M. Moran, eds., vol. 129, p. 169, (Jan., 1988).

[184] M.J. Reid et al., *The distance to the center of the galaxy: H2O maser proper motions in SGR B2(N)*, NASA STI/Recon Technical Report N, (Nov., 1987).

[185] K.Y. Lo, *Mega-Masers and Galaxies*, *Ann. Rev. Astron. Astrophys.* **43** (2005) 625.

[186] K. Hachisuka et al., *Water maser motions in w3(oh) and a determination of its distance*, *Astrophys. J.* **645** (2006) 337 [astro-ph/0512226] [INSPIRE].

[187] C.R. Gwinn, J.M. Moran and M.J. Reid, *Distance and Kinematics of the W49N H_2O Maser Outflow*, *Astrophys. J.* **393** (1992) 149.

[188] A.D. Haschick, W.A. Baan and E.W. Peng, *The Masering Torus in NGC 4258*, *Astrophys. J. Lett.* **437** (1994) L35.

[189] S.J. Wijnholds, S. van der Tol, R. Nijboer and A.-J. van der Veen, *Calibration Challenges for Future Radio Telescopes*, *IEEE Sig. Proc. Mag.* **27** (2010) 30 [arXiv:1004.0156] [INSPIRE].

[190] C.D. Huang et al., *Hubble Space Telescope Observations of Mira Variables in the Type Ia Supernova Host NGC 1559: An Alternative Candle to Measure the Hubble Constant*, arXiv:1908.10883 [INSPIRE].

[191] M.M. Rau, S.E. Koposov, H. Trac and R. Mandelbaum, *Calibrating Long Period Variables as Standard Candles with Machine Learning*, *Mon. Not. Roy. Astron. Soc.* **484** (2019) 409 [arXiv:1806.02841] [INSPIRE].

[192] W. Yuan, L.M. Macri, A. Javadi, Z. Lin and J.Z. Huang, *Near-infrared mira period-luminosity relations in m33*, *Astron. J.* **156** (2018) 112.

[193] T. Muraveva et al., *The carnegie rr lyrae program: mid-infrared period-luminosity relations of rr lyrae stars in reticulum*, *Mon. Not. Roy. Astron. Soc.* **480** (2018) 4138.

JCAP06(2022)002

[194] C.R. Klein, J.W. Richards, N.R. Butler and J.S. Bloom, *Mid-infrared Period-Luminosity Relations of RR Lyrae Stars Derived from the WISE Preliminary Data Release*, *Astrophys. J.* **738** (2011) 185 [*Erratum ibid.* **764** (2013) 110] [arXiv:1105.0055] [INSPIRE].

[195] A. Bhardwaj, S.M. Kanbur, L.M. Macri, H.P. Singh, C.-C. Ngeow and E.E.O. Ishida, *Large Magellanic Cloud Near-Infrared Synoptic Survey — III. A statistical study of non-linearity in the Leavitt Laws*, *Mon. Not. Roy. Astron. Soc.* **457** (2016) 1644 [arXiv:1601.00953].

[196] C.-C. Ngeow, S.M. Kanbur, S. Nikolaev, J. Buonaccorsi, K.H. Cook and D.L. Welch, *Further empirical evidence for the non-linearity of the period-luminosity relations as seen in the Large Magellanic Cloud Cepheids*, *Mon. Not. Roy. Astron. Soc.* **363** (2005) 831 [astro-ph/0507601] [INSPIRE].

[197] C. Ngeow, S. Kanbur and A. Nanthakumar, *Testing the nonlinearity of the BVI(c)JHK(s) period-luminosity relations for the Large Magellanic Cloud Cepheids*, *Astron. Astrophys.* **477** (2008) 621 [arXiv:0710.5128] [INSPIRE].

[198] W.L. Freedman and B.F. Madore, *An empirical test for the metallicity sensitivity of the Cepheid period-luminosity relation*, *Astrophys. J.* **365** (1990) 186 [INSPIRE].

[199] W.L. Freedman and B.F. Madore, *Two New Tests of the Metallicity Sensitivity of the Cepheid Period-Luminosity Relation (The Leavitt Law)*, *Astrophys. J.* **734** (2011) 46 [arXiv:1103.6235] [INSPIRE].

[200] M. Salaris and S. Cassisi, *The tip of the red giant branch as a distance indicator: results from evolutionary models*, *Mon. Not. Roy. Astron. Soc.* **289** (1997) 406 [astro-ph/9703186] [INSPIRE].

[201] S. Chandrasekhar and E.A. Milne, *The Highly Collapsed Configurations of a Stellar Mass*, *Mon. Not. Roy. Astron. Soc.* **91** (1931) 456 [INSPIRE].

[202] M.M. Phillips, *The absolute magnitudes of Type IA supernovae*, *Astrophys. J. Lett.* **413** (1993) L105 [INSPIRE].

[203] D. Branch and G.A. Tammann, *Type ia supernovae as standard candles*, *Ann. Rev. Astron. Astrophys.* **30** (1992) 359 [INSPIRE].

[204] M.M. Ivanov, Y. Ali-Haïmoud and J. Lesgourgues, *H0 tension or T0 tension?*, *Phys. Rev. D* **102** (2020) 063515 [arXiv:2005.10656] [INSPIRE].

[205] M. Bartelmann, *Gravitational Lensing*, *Class. Quant. Grav.* **27** (2010) 233001 [arXiv:1010.3829] [INSPIRE].

[206] S. Birrer and T. Treu, *Astrometric requirements for strong lensing time-delay cosmography*, *Mon. Not. Roy. Astron. Soc.* **489** (2019) 2097 [arXiv:1904.10965] [INSPIRE].

[207] S. Brough et al., *The Vera Rubin observatory legacy survey of space and time and the low surface brightness universe*, arXiv:2001.11067.

[208] P. Salucci et al., *Einstein, planck and vera rubin: Relevant encounters between the cosmological and the quantum worlds*, *Front. Phys.* **8** (2021).

[209] EUCLID collaboration, *Euclid preparation: I. The Euclid Wide Survey*, arXiv:2108.01201 [INSPIRE].

[210] O. Tihhonova et al., *H0LiCOW VIII. A weak-lensing measurement of the external convergence in the field of the lensed quasar HE 0435−1223*, *Mon. Not. Roy. Astron. Soc.* **477** (2018) 5657 [arXiv:1711.08804] [INSPIRE].

[211] V. Bonvin et al., *H0LiCOW — V. New COSMOGRAIL time delays of HE 0435–1223: H_0 to 3.8 per cent precision from strong lensing in a flat ΛCDM model*, *Mon. Not. Roy. Astron. Soc.* **465** (2017) 4914 [arXiv:1607.01790] [INSPIRE].

JCAP06(2022)002

[212] DES collaboration, *COSMOGRAIL: the COSmological MOnitoring of GRAvItational Lenses — XVI. Time delays for the quadruply imaged quasar DES J0408-5354 with high-cadence photometric monitoring*, *Astron. Astrophys.* **609** (2018) A71 [arXiv:1706.09424] [INSPIRE].

[213] LSST Dark Energy Science collaboration, *Strongly lensed SNe Ia in the era of LSST: observing cadence for lens discoveries and time-delay measurements*, *Astron. Astrophys.* **631** (2019) A161 [arXiv:1903.00510] [INSPIRE].

[214] LSST Science and LSST Project collaborations, *LSST Science Book, Version 2.0*, arXiv:0912.0201 [INSPIRE].

[215] S.W. Jha et al., *Next Generation LSST Science*, arXiv:1907.08945 [INSPIRE].

[216] LSST collaboration, *Science-Driven Optimization of the LSST Observing Strategy*, arXiv:1708.04058 [INSPIRE].

[217] G.-B. Zhao et al., *Dynamical dark energy in light of the latest observations*, *Nature Astron.* **1** (2017) 627 [arXiv:1701.08165] [INSPIRE].

[218] R.-Y. Guo, J.-F. Zhang and X. Zhang, *Can the H_0 tension be resolved in extensions to ΛCDM cosmology?*, *JCAP* **02** (2019) 054 [arXiv:1809.02340] [INSPIRE].

[219] W.-M. Dai, Y.-Z. Ma and H.-J. He, *Reconciling Hubble Constant Discrepancy from Holographic Dark Energy*, *Phys. Rev. D* **102** (2020) 121302 [arXiv:2003.03602] [INSPIRE].

[220] H.B. Benaoum, W. Yang, S. Pan and E. Di Valentino, *Modified emergent dark energy and its astronomical constraints*, *Int. J. Mod. Phys. D* **31** (2022) 2250015 [arXiv:2008.09098] [INSPIRE].

[221] L. Verde, J.L. Bernal, A.F. Heavens and R. Jimenez, *The length of the low-redshift standard ruler*, *Mon. Not. Roy. Astron. Soc.* **467** (2017) 731 [arXiv:1607.05297] [INSPIRE].

[222] T. Brinckmann and J. Lesgourgues, *MontePython 3: boosted MCMC sampler and other features*, *Phys. Dark Univ.* **24** (2019) 100260 [arXiv:1804.07261] [INSPIRE].

[223] D. Scolnic et al., *The Pantheon+ Analysis: The Full Dataset and Light-Curve Release*, arXiv:2112.03863 [INSPIRE].

[224] A. Carr et al., *The Pantheon+ Analysis: Improving the Redshifts and Peculiar Velocities of Type Ia Supernovae Used in Cosmological Analyses*, arXiv:2112.01471 [INSPIRE].

[225] K. Krisciunas et al., *The Carnegie Supernova Project I: Third Photometry Data Release of Low-Redshift Type Ia Supernovae and Other White Dwarf Explosions*, *Astron. J.* **154** (2017) 211 [arXiv:1709.05146] [INSPIRE].

[226] S.L. Hoffmann et al., *Optical Identification of Cepheids in 19 Host Galaxies of Type Ia Supernovae and NGC 4258 with the Hubble Space Telescope*, *Astrophys. J.* **830** (2016) 10 [arXiv:1607.08658] [INSPIRE].

[227] A. Bhardwaj et al., *Large Magellanic Cloud Near-infrared Synoptic Survey. II. The Wesenheit Relations and Their Application to the Distance Scale*, *Astron. J.* **151** (2016) 88 [arXiv:1510.03682].

[228] B.F. Madore, *The period-luminosity relation. IV. Intrinsic relations and reddenings for the Large Magellanic Cloud Cepheids*, *Astrophys. J.* **253** (1982) 575.

[229] Pan-STARRS1 collaboration, *The Complete Light-curve Sample of Spectroscopically Confirmed SNe Ia from Pan-STARRS1 and Cosmological Constraints from the Combined Pantheon Sample*, *Astrophys. J.* **859** (2018) 101 [arXiv:1710.00845] [INSPIRE].

[230] J. Lesgourgues, *The Cosmic Linear Anisotropy Solving System (CLASS) I: Overview*, arXiv:1104.2932 [INSPIRE].

JCAP06(2022)002

[231] C.L. Steinhardt, A. Sneppen and B. Sen, *Effects of Supernova Redshift Uncertainties on the Determination of Cosmological Parameters*, *Astrophys. J.* **902** (2020) 14 [arXiv:2005.07707] [INSPIRE].

[232] J. Lesgourgues and S. Pastor, *Massive neutrinos and cosmology*, *Phys. Rept.* **429** (2006) 307 [astro-ph/0603494] [INSPIRE].

[233] S. Hannestad, *Neutrino physics from precision cosmology*, *Prog. Part. Nucl. Phys.* **65** (2010) 185 [arXiv:1007.0658] [INSPIRE].

[234] R.-G. Cai, Z.-K. Guo, L. Li, S.-J. Wang and W.-W. Yu, *Chameleon dark energy can resolve the Hubble tension*, *Phys. Rev. D* **103** (2021) 121302 [arXiv:2102.02020] [INSPIRE].

[235] X. Li and A. Shafieloo, *A Simple Phenomenological Emergent Dark Energy Model can Resolve the Hubble Tension*, *Astrophys. J. Lett.* **883** (2019) L3 [arXiv:1906.08275] [INSPIRE].

[236] M. Raveri and W. Hu, *Concordance and Discordance in Cosmology*, *Phys. Rev. D* **99** (2019) 043506 [arXiv:1806.04649] [INSPIRE].

[237] A.G. Riess, S. Casertano, W. Yuan, L.M. Macri and D. Scolnic, *Large Magellanic Cloud Cepheid Standards Provide a 1% Foundation for the Determination of the Hubble Constant and Stronger Evidence for Physics beyond ΛCDM*, *Astrophys. J.* **876** (2019) 85 [arXiv:1903.07603] [INSPIRE].

[238] P. Lemos, E. Lee, G. Efstathiou and S. Gratton, *Model independent $H(z)$ reconstruction using the cosmic inverse distance ladder*, *Mon. Not. Roy. Astron. Soc.* **483** (2019) 4803 [arXiv:1806.06781] [INSPIRE].

JCAP06(2022)002